

Octopus: Scalable Low-Cost CXL Memory Pooling

Daniel S. Berger
Microsoft Azure
University of Washington
Redmond, USA

Yuhong Zhong
Columbia University
Microsoft Azure
New York, USA

Fiodar Kazhamiaka
Microsoft Azure
Redmond, USA

Pantea Zardoshti
Microsoft Azure
Redmond, USA

Shuwei Teng
Microsoft Azure
Redmond, USA

Mark D. Hill
University of
Wisconsin-Madison
Madison, USA

Rodrigo Fonseca
Microsoft Azure
Redmond, USA

Abstract

Compute Express Link (CXL) enables compute “pods” with memory pooling across hosts to reduce cost and improve efficiency. Existing pods are small, use exotic many-ported pooling devices, or require indirection through expensive switches. These conventional designs implicitly assume that pods must fully connect all hosts to all CXL pooling devices.

This paper breaks with this conventional wisdom to create “Octopus” pods. Octopus connects each host to a bounded number of pooling devices (e.g., 8), each pooling device connects to different subsets of hosts, and all host pairs share at least one pooling device. Despite no longer having a global memory pool, we show that Octopus pods still effectively support memory pooling, as well as various communication patterns. Relative to conventional pods, Octopus is more cost-effective (using near-commodity pooling devices) and enables larger pods (allowing more pooling flexibility and greater communication reach).

Simulations on production traces show Octopus achieves memory savings comparable to expensive pool designs. Hardware experiments confirm that Octopus reduces RPC latency by $3\times$ compared to RDMA. Our work formalizes Octopus topologies, develops memory allocation algorithms, and evaluates performance tradeoffs through simulation and hardware testing.

CCS Concepts: • Computer systems organization → Cloud computing.

Keywords: Cloud Architecture, Memory Pooling, CXL

1 Introduction

Memory scaling limits [26, 59, 82] are broadly affecting cloud platforms today. For example, Microsoft Azure and Meta report that DRAM can account for half of server cost [65, 76]. Creating pods that pool memory across hosts promises to significantly lower memory costs [2, 26, 58, 65, 105, 112]. Another challenge arises in distributed systems, where networking latency imposes significant overheads [30, 66, 89, 114]. Sharing memory across hosts in a pod can overcome

these bottlenecks by enabling low-latency communication between nodes [8, 30, 66, 73, 75, 89, 114–116].

A promising technology to enable these memory pods is the Compute Express Link (CXL), an open interconnect standard that connects processors with memory pools and other devices [24]. CXL provides memory semantics with bandwidth that scales with PCIe while achieving latency within $\approx 2\times$ the access latency of local memory. Major CPU vendors, device manufacturers, and datacenter operators have adopted CXL as a common standard [24, 65].

The design space for CXL pod architectures remains largely open. We are aware of three approaches to build a pod. First, one may use small pooling devices (PDs) with two to four ports and $\approx 250ns$ latency that are available as a near-commodity today [16, 40, 54, 77]. Second, one may use large PDs (8-16 ports), but these have much higher costs (6-19 \times) and limited availability. The promise of wide availability of these devices [25, 36, 38, 43, 65, 74, 104] has not yet materialized. Third, one may use CXL switches with up to 32 ports. However, switches require multiple serialization-deserialization steps, which results in high latencies of 500–600ns in the few existing prototypes [45, 70]. Besides their latency overhead, prior work showed that the cost of switch-based pod designs are likely far too expensive [9, 64].

Industry widely believes that pods will deploy with direct connections to multi-port PDs [25, 36, 38, 43, 65, 74, 90, 104]. A common assumption is that pods require a *fully-connected topology* where every host is connected to every PD, and every PD is connected to every host. Thus, the PD port count determines the pod size. This has hindered real-world deployment since small PD port counts limit the pod size, and large PDs are expensive and rare.

This paper proposes an unconventional CXL pod design, Octopus. Our key insight is that a *fully-connected topology is not needed for most use cases*, enabling cost-effective designs. We find that dynamic memory allocation (resource pooling) benefits from a “power of two choices effect” similar to load balancing [79]. Perfectly balancing within a pod matters less

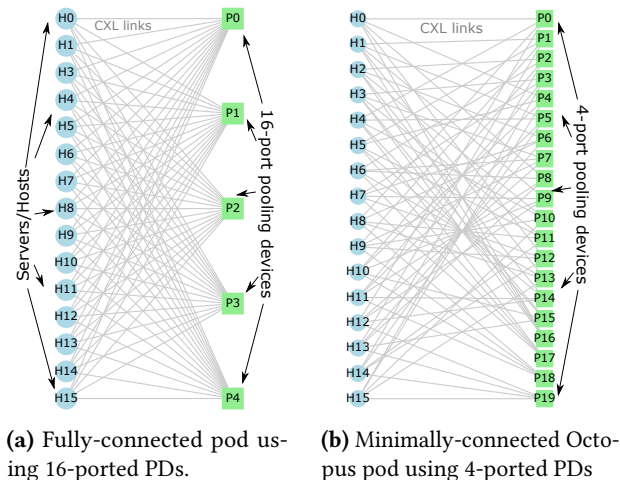


Figure 1. Conventional CXL pod designs assume that all 16 hosts (H_0 to H_{15}) connect to all pooling devices, which requires a still-expensive 16-ported device. Octopus introduces minimally-connected pod designs based on near-commodity 4-port pooling devices, which cuts pooling device cost in half.

than the overall pod size. Similarly, we find that communication largely requires pair-wise memory sharing. We propose *minimally-connected* and *redundantly-connected* pod topologies. They exploit the fact that hosts have multiple CXL ports, e.g., eight $\times 8$ ports on Xeon 6 platforms [47, 49, 62, 87, 99]. In Octopus, a host is *not connected to every PD, but all hosts share access to at least one common PD*. For example, an Octopus pod reaches 16 hosts while using 4-port PDs, which reduces CXL overhead costs by $2.1\times$ compared to large 16-port PDs required for a comparable fully-connected pod (Figure 1). Alternatively, given 4-port PDs, an Octopus pod can reach 25 hosts compared to just 4 hosts in a fully-connected pod.

Octopus introduces a trade-off: hosts can access only subsets of overall pod memory. We find this mainly affects broadcast communication primitives optimized for a single shared buffer. For the large set of remaining use cases, we introduce a software stack that effectively mitigates this trade-off.

We evaluate Octopus through a mixture of methods. We formally prove that the Octopus’s memory allocation algorithm can match the memory savings achieved by a large (and expensive) PD at the same pod size. We validate this analysis with simulations for three sets of production traces from Microsoft. We experimentally validate pair-wise communication latency using real hardware. Octopus matches the latency of fully-connected topologies while reducing RPC latency by $3.25\times$ compared to RDMA.

Octopus pod topologies present a surprisingly rich design space, which we formalize using combinatorial design theory. This approach enables the parametrized construction of topologies where any pair of hosts can share access

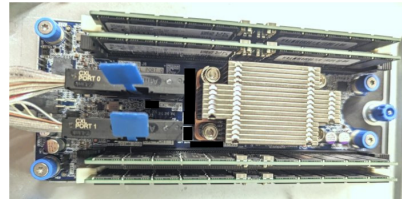


Figure 2. Multi-ported device with two CXL ports. Each port offers $\times 8$ CXL lanes.

to one PD (minimally-connected Octopus) or multiple PDs (redundantly-connected Octopus).

This paper makes the following technical contributions.

- First paper to question the assumption that pods must fully-connect hosts and pooling devices
- Propose Octopus pod designs with bounded connections and provide algorithmic constructions for minimally and redundantly-connected topologies.
- Quantification of design constraints in CXL pooling device design
- Memory allocation and buffer placement algorithms for Octopus topologies
- Quantitative evaluation of Octopus’s benefits and trade-offs through analysis and hardware experiments

2 CXL Background and Use Cases

2.1 CXL Overview

The Compute Express Link (CXL) interconnect standard itself is described in detail in a recent tutorial [24]. Octopus focuses on the CXL.mem protocol in which CPUs forward ld/st instructions to a CXL memory controller based on the address range.

A CXL controller typically offers multiple DRAM channels, which can be DDR4 or DDR5. A single CPU typically has multiple CXL ports. For example, Intel Xeon 6 (Granite Rapids) production platforms typically use 64 CXL lanes per CPU socket, e.g., [47, 49, 62, 87, 99]. These lanes are configurable as four $\times 16$ CXL or eight $\times 8$ CXL ports.

We call a CXL controller with more than one CXL port a *pooling device* (PD). PDs enable multiple CPUs to connect to the same controller and access its memory. These devices are available today. Figure 2 shows a PD with two $\times 8$ CXL ports. Other examples include devices by AстераLabs [54], Marvell [77], the Hyperscale CXL OpenCompute specification led by Meta and Google [16], and xFusion [40].

PDs connect to the CPU’s CXL ports with physical PCIe pins and cables. In our signal integrity models and lab experiments, copper CXL cables reach around 80cm (Section 5). Longer cables require a retimer or active cables, which adds latency and power consumption. For example, the AстераLabs Aries module advertises 7m reach while adding 10ns and 11W [5].

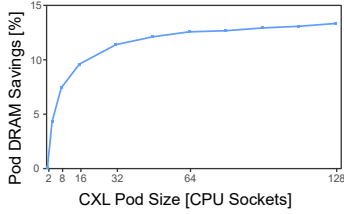


Figure 3. Larger CXL pods lead to higher DRAM savings.

Besides PDs, another approach to build a pool is a switch. Switches offer multiple CXL ports and can forward CXL packets between them. An example is the XC50256 CXL switch offered by XConn [110].

A CXL pod comprises multiple hosts using multiple PDs and/or switches. In principle, hosts can concurrently access the memory behind a PD or behind a switch. However, while CXL standards after 3.0 introduce optional hardware coherence, neither currently-available CPUs nor pooling devices support this feature.

2.2 CXL Pod Use Cases

Prior work has proposed and continues to propose a variety of use cases for CXL pods. We categorize these use cases into three broad categories: resource pooling, memory sharing between pairs of hosts, and pod-wide memory sharing.

Dynamic Memory Allocation. Resource pooling involves allocating CXL pod capacity to hosts for exclusive access and dynamically changing this allocation over time. Specific use cases include improving application performance by adding more memory [33], reducing memory cost by multiplexing memory demands across cloud hosts [65, 105], lower cost and higher performance in in-memory databases [2, 58], and lower cost for serverless function platforms [112].

In CXL, dynamic allocation is implemented at a block size called extents [24, 65]. Importantly, memory is treated as a capacity resource, i.e., hosts do not typically care which extent is allocated to them. This enables significant flexibility in the pod memory allocation algorithm, which we further discuss in Section 5.

Sharing Memory between Pairs of Hosts. We find that most existing use cases for CXL shared memory involves sharing memory between pairs of hosts or small subsets of the pod. A common use case for CXL pods is fast RPCs [8, 73, 75, 115, 116]. Even complex communication patterns typically are implemented based on message-passing interfaces [17, 22, 71, 95]. For example, production AllGather implementations are based on ring algorithms [7, 22, 86]. All of these implementations require sharing memory only between pairs of hosts.

A second use case for CXL pod is remotely accessing PCIe devices such as NICs, SSDs, or accelerators [118]. Again this requires CXL-based communication channels between the

host accessing the device and the host where the device is physically attached.

A third set of use cases focuses on fail-over between hosts. Typically, these use cases target databases and rely on variants of primary-backup replication [18, 78, 83, 101, 116, 119]. Primary-backup [46, 69] involves pair-wise communication between the primary and backup hosts.

Distributed consensus also falls into this category. Many consensus algorithms are leader based and involve pair-wise communication between the leader and all other hosts such as Viewstamped Replication [68], Zookeeper [42], Raft [85], and HotStuff [113]. Some CXL-based distributed transaction system proposals also involve a central coordinator, such as a transactional CXL controller [32]. Some Paxos variants can be considered leaderless; however they also involve pair-wise communication between each proposer and acceptor [56].

Shuffle operations are widely-used in distributed analytics, and often cited as a key use case for CXL shared memory [6, 8, 35, 63, 101, 107]. For example, Memverge has shown 2.8× shuffle speedups in a prototype [101]. One might expect that performing distributed shuffle operations in CXL shared memory would require sharing memory between all pod hosts. However, we will show an efficient pair-wise shuffle design in Section 5.

Sharing Memory between All Pod Hosts. The primary use case for pod-wide memory sharing today are optimized variants of broadcast communication that do not rely on message passing. A host could write its broadcast data into a PD once and other hosts could read it directly from this PD. The same principle applies to shared-memory AllGather [1].

Besides broadcast variants, we are only aware of one other use case that requires pod-wide memory sharing: distributed transactions that are directly implemented within CXL without requiring message passing [41]. However, CXL transactions require synchronization primitives or hardware coherence that are not yet supported by existing CXL 2.0 hardware including CPUs and pooling devices.

2.3 Common Use Case Requirements

We find three common requirements. First, use cases require *low access latency* to CXL pod memory. Recent work has found that CXL-related application slowdowns deteriorate super-linearly as CXL access latency increases [70].

Second CXL use cases require *low-cost* access to CXL pods. As many use case implementations are still being developed, they are highly cost-sensitive until they realize their full potential.

Third, use case benefit from *large CXL pod sizes*. For example, in dynamic memory allocation, larger CXL pod sizes translate into higher memory savings due to multiplexing memory demands across more hosts. Figure 3 visualizes this

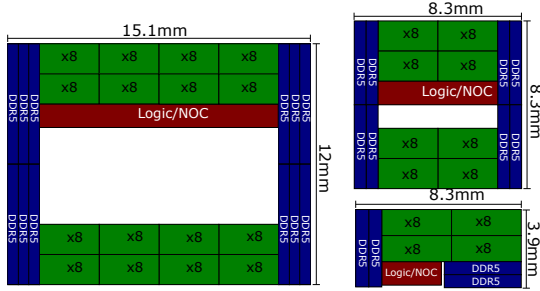


Figure 4. Die area estimates for PDs with different numbers of CXL ports and DDR5 channels. Note that for visual simplicity we show the logic and network-on-chip (NOC) area as a single block.

PD Size	$N = 2$	$N = 4$	$N = 8$	$N = 16$
DDR5 channels	2	4	8	12
References	[40, 54, 77]		[38]	[81]
Overall die area	14 mm^2	30 mm^2	69 mm^2	181 mm^2
Dead silicon	0 mm^2	2 mm^2	12 mm^2	77 mm^2
Wafer cost	70%	80%	100%	150%
Estimated cost ^a	\$260	\$590	\$1,500	\$5,000

Table 1. Cost estimates for different PDs sizes derived from die area estimates (Figure 4) and simple cost modeling [97].

for Microsoft Azure cloud hosts [9]. Fast RPCs, general communication, fail-over, shuffle, and broadcast use cases also benefit from larger pod sizes.

3 CXL Building Blocks and Existing Designs

We review existing pooling device (PD) and pod designs that motivate our design proposal in Section 4. Multi-ported CXL PDs form a key building block for Octopus pods.

3.1 Pooling Device Costs

We estimate hypothetical PD costs by estimating die area and using a literature cost model that accounts for IO-pad-limited dies [97]. Specifically, we consider PDs that use $N = 2, 4, 8, 16$ CXL ports with each port using $\times 8$ lanes. Figure 4 shows our die area estimates which scale superlinearly with port count. This is partly due to being IO-pad limited and due to different volume assumptions leading to different wafer costs. Appendix B contains the details of our cost model, while resulting cost estimates are shown in Table 1. For example, we find that $N = 2$ -port PDs cost about 5% as much as $N = 16$ -port PDs while offering 13% of the port count. This motivates our use of small port-count PDs in Octopus.

3.2 Existing CXL Pod Designs

Existing literature proposes either switched CXL pod designs or fully-connected CXL pods based on multiported pooling devices.

3.2.1 Switched CXL Pods. Any CXL controller (including a single-ported controller) may be connected to a CXL switch, which in turn connects multiple CPUs. Switched designs resemble tree network topologies in CXL 2.0 [48] and Clos network topologies in CXL 3.0 [80]. A single switch typically offers 128-256 CXL lanes [110]. These lanes would be shared among connected CPUs, CXL controllers, and other devices. For example, 128 lanes could connect six CPUs with $\times 16$ CXL ports and two single-ported CXL controllers with $\times 16$ ports. CXL 3.0 may support multiple switching levels [24].

The tradeoff for switched designs is higher power, cost, and latency. Prior work observes that CXL switch costs can exceed the benefits that can be achieved from pooling at scale [9, 64]. CXL switch latency is also fundamentally higher than direct CXL connections, as switches require serialization and deserialization of CXL packets twice on every path from CPU to CXL memory controller [9, 65]. Current switches add more than 250ns of latency [45], resulting in idle load-to-use latency of roughly 500 – 600ns.

3.2.2 Fully-connected CXL Pods based on Multi-Ported Devices.

The alternative to switched CXL pods is connecting CPUs directly to PDs [65]. To our knowledge, all existing proposals assume a fully connected topology where every PD connects to every host. For example, as shown in Figure 1 five 16-ported PDs connect to the same 16 CPUs. Fully-connected topologies have been proposed in official CXL standard presentations by Microchip and Intel [104], and in industry presentations by Seagate [25], ARM [38], SK Hynix [36], Microsoft [65], Jackrabbit labs [74], and Unifabrix [43]. The common assumption is that N -ported PDs will create a CXL pod of N CPUs. Every CPU in the pod connects to the same set of X PDs. All CPUs can access and allocate memory from any of the X PDs in the pod.

Compared to switched topologies, large PDs reduce cost, power, and latency [9]. However, we find that we can further improve cost and latency by *changing the pod topology*.

4 Octopus Overview and Foundations

Octopus introduces a novel class of CXL pod designs for small PDs that increases the number of inter-connected hosts (the pod size). The design space for Octopus topologies is inherently large, offering potential for co-designing specific network topologies tailored to particular applications. In this work, we focus on two generalized classes of pod designs. The first class connects each pair of hosts directly to exactly one PD, enabling efficient pair-wise sharing and low-latency RPCs among any two connected hosts. The second class introduces redundancy by connecting every pair of hosts to

two PDs. Redundancy makes the topology more robust and enables higher-bandwidth communication between hosts.

4.1 Connectivity

Central to Octopus’s feasibility is the observation that every host provides $X > 1$ independent CXL ports, allowing each host to connect simultaneously to multiple PDs. Current hardware offers $X = 8$ ports per host (Section 2). Multiple host ports enable each host to connect to multiple PDs which in turn connect to different subsets of hosts. For simplicity, we assume single-socket servers¹ where each CPU constitutes a distinct host.

We illustrate examples of fully-connected (FC) and Octopus topologies in Figure 1. Given $N = 16$ -ported PDs and $X = 5$ host ports, a FC pod spans 16 hosts. Octopus can achieve the same pod size of 16 hosts using $N = 4$ -ported PDs. For the more common case of $X = 8$ and $N = 4$, Octopus can span 25 hosts. Appendix A visualizes these larger topologies.

4.2 Memory provisioning

Fully-connected pods can maximize savings from dynamic memory allocation by multiplexing memory demand across the entire pool. Since memory can be allocated from any host to any pooling device, the amount required for the pod is the *average per-host CXL utilization*. In contrast, Octopus pods expose a subset of total pool memory to each host. Thus, it may not be possible to satisfy a set of host demands even if there is sufficient total memory capacity across all pooling devices. This can happen if there are particularly skewed demand distributions across hosts, e.g., a subset of hosts whose total demand exceeds the capacity available across pooling devices connected to these hosts.

To motivate the overall design of Octopus, we formally prove under which conditions a minimally-connected topology requires *extra memory compared to the average* required for a fully-connected topology. We then empirically verify that in practice host memory demands meet the condition under which Octopus does not need this extra memory. Thus, Octopus is near optimal for memory provisioning despite its key limitation of only making subsets of its pod memory available to hosts. The following theorem formally describes an upper bound on the extra memory required.

Theorem 4.1. *Given a minimally-connected Octopus pod with H hosts, X ports per host, and N ports per PD, and a set of host memory capacity demands D_1, \dots, D_H . Let μ be the average CXL memory demand across hosts ($\mu = \sum_{i=1}^H D_i / H$) and let $D_{(1)}, D_{(2)}, \dots, D_{(H)}$ be the host demands sorted in non-increasing order.*

¹Octopus topologies also apply to multi-socket servers. In this case, we still seek to connect pairs of CPU sockets with each other. However, we incorporate the cache-coherent processor interconnection network to reduce required CXL links.

The memory capacity required for the Octopus pod is bounded by the following:

$$\text{MemCap} \leq \alpha \cdot \mu \cdot H \quad (1)$$

when α satisfies the following condition for all $k = 1..H$:

$$\sum_{i=1}^k D_{(i)} \leq \alpha \cdot \frac{k \cdot N \cdot X}{X + k - 1} \mu$$

A proof of this theorem – provided in Appendix C – is based on a counting argument combined with a Cauchy-Schwarz inequality, and exploits the minimally-connected property of Octopus pools. Note that $\mu \cdot H$ is the capacity required by a fully-connected topology; the factor α bounds the additional memory required for a minimally-connected Octopus pod.

Section 5 describes in detail how to construct Octopus topologies and how they map to physical rack designs. Section 6 describes the Octopus software stack. In Section 7, we use production traces from several workloads to show that low values of α satisfy the theorem condition.

5 Octopus Hardware Design

An Octopus design comprises a logical network topology (Section 5.1) and a physical layout (Section 5.2). The logical topology represents the links between hosts and pooling devices. This topology ensures feasibility for host port and PD port constraints. The physical layout maps the logical topology to an actual server and rack design. This layout ensure feasibility of mechanical and signal integrity constraints.

5.1 Logical Network Topology

We focus on two classes of logical topologies. In a *minimally-connected* Octopus topology *every pair of hosts in the CXL pod connects to exactly one PD*. This enables single-hop communication throughout the CXL pod and allows basic balancing memory demands from hosts (Theorem 4.1). In a *redundantly-connected* Octopus topology *every pair of hosts connects to multiple PDs*. Redundancy facilitates robustness and scales up bandwidth between host pairs.

Increasing the degree of redundancy yields topologies that look increasingly closer to fully-connected topologies. In contrast, the design space of topologies that are sparser than minimally-connected is less well explored. We briefly discuss sparse topologies in Section 8.

We represent the logical topology as a bipartite graph with hosts as nodes on one side and PDs as nodes on the other side. CXL cables are represented as edges. The graph is uniquely defined given the number of host ports, X , the number of PD ports, N , and our requirements on pair-wise connectivity.

Minimally-connected Octopus topologies. For minimal connectivity, we require that every host must reach any other host node after traversing exactly two edges, first an edge

to a pool node and then an edge to the target host node. Additionally, if two host nodes connect to the same pool node, they cannot both connect to another pool node.

This topology leads to pods of size $H = 1 + X \times (N - 1)$. This is because any one host (say host A) connects to X different PDs. Every PD, has N ports, and one is already taken by host A . Thus, every PD can connect to $(N - 1)$ other hosts. So, host A shares a PD with $X \times (N - 1)$ other hosts, and we add host A itself into the pod size count. For typical X and N that are a power of two and greater than one, this always leads to *odd* pod sizes. This aspect is further discussed in Section 8.

The number of PDs to construct an Octopus topology is $M = \frac{H \times X}{N}$. We typically normalize the PD count by the number of hosts (which is indicative of costs at scale). The PD to host ratio is $\frac{X}{N}$. Note that this exactly matches the ratio in a fully-connected topology given the same X and N .

We formalize the construction of a minimally-connected Octopus topology as a balanced incomplete block design (BIBD) [14, 28, 96]. BIBD is a classical combinatorial design for statistical experiments [14, 28, 96]. Specifically, a minimally-connected Octopus topology is a $2 - (H, N, 1)$ BIBD. The first number qualifies that our constraints target pairs of hosts. The last number, $\lambda = 1$, defines the constraint on pairs of hosts connecting to exactly one common PD. Constructing BIBDs is NP hard [21] except for specific cases like $X = N$ [11]. There are usually many solutions to a $2 - (H, N, 1)$ BIBD. However, not all of them have favorable properties for CXL pod designs. For example, we require that hosts are well connected to each other in the same pod, which can be formally stated as requiring the BIBDs to be not partitionable. We also impose symmetry requirements, for easy of construction and practical implementations. Appendix A introduces a construction approach that fulfills these requirements and provide code to construct these topologies efficiently.

Redundantly-connected Octopus topologies. These topologies guarantee that every pair of hosts connects to exactly two PDs. A good model for redundantly-connected topologies is that we construct two different minimally-connected topologies given half the number of host ports ($X/2$) and then connect each host to both topologies. This makes it clear that a redundantly-connected topology leads to pods of size $H = 1 + \frac{X}{2} \times (N - 1)$.

Construction of these topologies follows the general approach outlined for minimally-connected ($\lambda = 1$) topologies, except for $\lambda = 2$. Formally, they are a solution to a $2 - (H, N, 2)$ BIBD. We again impose the same constraints and add an additional constraint that any triplet of hosts connects only in a single PD. Appendix A introduces a construction approach and code that fulfills these requirements.

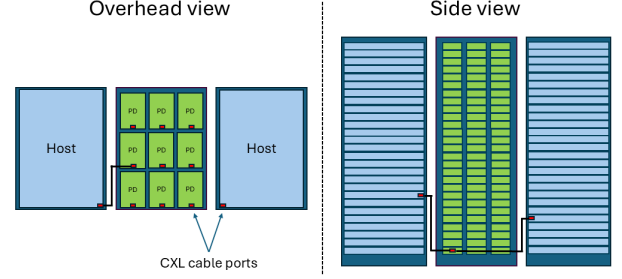


Figure 5. A 3-rack Octopus configuration.

5.2 Physical Layout

The physical layout of an Octopus topology is largely driven by CXL cable lengths and cable routing. CXL 2.0 (PCIe5) systems are typically constrained by insertion loss, which admits a simplified analysis. Under a 36 dB insertion-loss budget at 16 GHz, we allocate 8 dB for pad-to-pin (root complex) and 10 dB for the CXL pooling device. We conservatively allocate 10 dB for motherboard and connectors, since materials have a significant impact. This leaves 8 dB for cables, of which we allocate 3 dB for internal cabling at the memory pool chassis. Assuming AWS 29 Turbotwin unjacketed cable loss of 6 dB/m, this yields roughly 80 cm of external cable between server chassis and CXL pool. This roughly matches the results from prior analysis [91, 100].

Given a constraint of 80 cm cables, we propose a specific rack design to enable large logical pod topologies. Specifically, we propose 3-rack pod designs where compute hosts are located in the left and right racks, whereas pooling devices are located in the middle rack. Figure 5 sketches this design. Depending on the PD size (e.g., $N = 2$ vs $N = 16$), the middle rack can hold a varying number of PDs per rack slot. Assuming standard 19" datacenter racks, the dimension of each rack slot is approximately $1000 \times 600 \times 50$ mm.

To further optimize cable lengths, we assume compute hosts where CXL edge connectors are located at a front corner of the server chassis, directly on the motherboard. This is a similar requirement to those imposed by the OCP NIC 3.0 specification [84] which also requires PCIe5 ports at the front of the server. Based on existing designs (Figure 2), we assume that CXL ports on the PD side are in the front-middle of each PD.

We validate achievable topologies with and without re-timers in Section 7.

6 Octopus Software Design

The Octopus software stack spans firmware that controls how CXL memory is exposed to the OS, dynamic memory allocation algorithms, and buffer allocation for memory sharing.

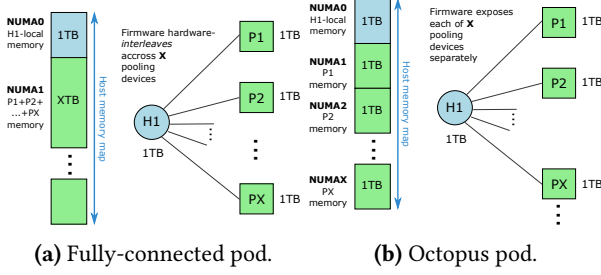


Figure 6. Host software view in fully-connected and Octopus pods.

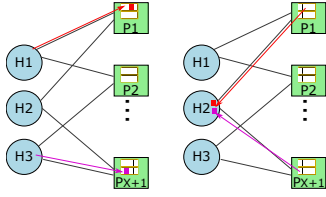


Figure 7. Pair-wise message passing and shuffle

6.1 Software CXL Pod API

In a fully-connected topology, memory is interleaved across CXL PDs by default. Specifically, CXL specifies hardware interleaving at 256 Byte granularity across CXL devices connected to a CPU socket [20].² Figure 6a shows the host memory map in a typical fully-connected topology.

Octopus makes individual CXL ports visible to the Operating System as separate NUMA nodes. Specifically, we modify firmware to disable 256B hardware interleaving across CXL devices. Figure 6b shows the resulting host memory map: each host sees $X + 1$ NUMA nodes (per CPU socket), one for local memory, and one for each connected pooling device.

By exposing every PD as a separate NUMA node, Octopus enables memory allocation from an explicit target PD. Explicitly addressing a PD allows balancing memory allocations across PD in dynamic memory (resource pooling) use cases (Section 6.2). Explicit addressing also facilitates memory sharing with specific hosts that connect to a known PD (Sections 6.3 - 6.4).

Octopus also requires hosts to understand the overall pod topology. In a hyperscale datacenter, a control plane assigns each host a unique identifier [37, 102] and performs high-level resource allocation functions. This control plane communicates pod configuration to each host.

²Note that CXL port interleaving is different from heterogeneous memory interleaving between local host DRAM and CXL memory; the interleaving policies described here exclusively consider interleaving among CXL devices [24].

6.2 Dynamic Memory Allocation

In fully-connected topologies, memory allocation is straightforward with the entire pod capacity represented as a single pool of memory.

In Octopus topologies, hosts allocate memory from a subset of PDs (those reachable to a given host), represented as NUMA nodes. There are two key factors in deciding which NUMA node to allocate memory from. First, we seek to avoid the situation that a host cannot allocate CXL pod capacity because its subset of PDs ran out of memory, while other PDs do have available memory. The goal of a Octopus memory allocation algorithm is thus to balance memory capacity demands across PDs (Theorem 4.1). Octopus uses a greedy balancing algorithm: allocate from the PD with the highest available capacity. We additionally rely on memory defragmentation where each host reallocates memory pages from PDs with lowest available capacity to PDs with highest available capacity, until all reachable PDs have equal available capacity. In practice, defragmentation is already necessary to align with extent boundaries (Section 2); so, Octopus’s defragmentation policy can be implemented by adding rules to these existing systems.

A second factor in memory allocation are memory bandwidth demands. While bandwidth requirements of most general-purpose cloud applications can be satisfied by a single $\times 8$ CXL link [9], some applications require more bandwidth. Octopus uses software-based interleaving policies that interleave memory across PDs at (4kB or 2MB) page granularity. To facilitate PD load balancing and defragmentation, Octopus seeks to use the smallest number of PDs for each application that satisfies its bandwidth demands. We thus continuously monitor application bandwidth requirements and adapt software interleaving to these demands.

6.3 Sharing Memory between Pairs of Hosts

All Octopus topologies support memory sharing between any pair of hosts.

We use pair-wise memory sharing to implement communication queues between pairs of hosts. Each host uses message input queues on every PD it is connected to. It dedicates a thread to continuously poll all these input queues³. Figure 7 sketches this scenario for a case where H1 and H3 seek to both send messages to H2, using PD1 and P(X+1), respectively. We evaluate the latency of an RPC implementation on top of these message buffers in Section 7.

Our distributed shuffle implementation works similarly to pair-wise communication. Shuffle involves every host sending data chunks to a specific target host, and receiving data chunks from other hosts. Thus, we use the same concept of input queues. At the beginning of shuffle, every host writes

³Since current CXL 2.0 CPUs and PDs do not support hardware coherence, polling involves a loop that flushes all cachelines and prefetches/reads from all input queues.

its shuffle data to the respective input queues. Once done writing, every host reads all of its input queues. We evaluate the completion time of shuffle in Section 7.

6.4 Sharing Memory between All Pod Hosts

Sharing memory between *all* hosts in a pod is generally not well supported Octopus topologies. For example, a single-shared-buffer Broadcast or AllGather implementation on CXL [1] would only require every broadcaster to write its data once, in a fully-connected topology. In Octopus, we functionally replicate broadcast by having each broadcaster write its data to all of its connected PDs. This write amplification makes an Octopus implementation less efficient than fully-connected topologies. We quantify this tradeoff in Section 7.

7 Evaluation

Our evaluation of Octopus CXL pod designs focuses on three broad questions.

How does cost scale with pod size for traditional and Octopus designs? *We find that Octopus achieves a 2× cost reduction at equal pod size, or a 4.5× larger topology at equal cost, compared to FC topologies.*

Can Octopus match the memory savings of an equally-sized fully-connected (FC) pod? *We find that Octopus achieves almost always the same memory savings as a FC pod.*

What are the implications of our design for memory-sharing use cases such as pair-wise communication, shuffle, and broadcast? *Octopus works well for pair-wise communication and shuffle, but has significantly longer broadcast completion times than FC topologies.*

7.1 Evaluation Setup

Octopus parameters. The design space for Octopus topologies is large. Our evaluation particularly focuses on minimally-connected topologies ($\lambda = 1$). As described in Section 2, it is common today for hosts to connect to devices using 64 CXL 2.0 / PCIe5 lanes. Given a $\times 8$ connection, this means that each host can typically connect to $X = 8$ PDs. Appendix A describes how to construct these topologies and other variants in detail. Unless otherwise noted, we evaluate a minimally-connected Octopus pod with 25 hosts and 25 PDs, each with 8 ports; we refer to this topology as *Octopus-25*.

Cost model. To model the cost overhead of CXL, we assume a hyperscale scenario where a large number of racks adopt CXL. While the purchase cost of a smaller CXL pod may be lower than a larger CXL pod, a hyperscaler will have to buy proportionally more of the smaller CXL pods. We assume a server purchase cost of \$10k and the estimated cost per PD from Table 1. To estimate cost savings from pooling, we assume that 50% of server purchase cost comes from DRAM, following prior work [65].

Physical layout model. We validate the physical realization of a given Octopus topology within the 3-rack layout (Section 5) under CXL cable length constraints by modeling server and PD placement as a satisfiability (SAT) problem. Each potential host and PD location within the racks is modeled as a 3-D coordinate that specifies the location of the ports for each host/PD slot. For large topologies where the host count exceeds the available rack slots, we model two hosts sharing a rack slot, with half-slot host ports located at the edge of the slot from that is closest to the PD rack.

The cable length limit is modeled as a three-dimensional Manhattan distance between host and PD ports, and is enforced through constraints on the one-to-one mapping of logical PD and host pairs – as defined by a given logical topology – to physical locations in the racks. Specifically, if logical PD i and host j are connected in the topology, any physical pair of PD α and host β that have a Manhattan distance greater than the cable length must not both be mapped to i and j , i.e., $\neg(i \rightarrow \alpha) \vee \neg(j \rightarrow \beta)$. If a mapping that satisfies the constraints is found, then the mapping should be realizable physically, modulo cabling complexity. We implement the model in PySAT [44] and use MiniSat2.2 to solve.

Simulations. Our simulations play back three different types of production traces. We collected trace data over a two-week period in December 2024 from thousands of cloud VMs, serverless workloads, and database nodes across a subset of server in popular clusters at Microsoft. For each entity, we recorded allocation and deallocation times, resource allocation, and the server hosting the workload. We assume that a pod’s overall memory comprises 50% of host-local memory and 50% of PD-attached memory, which is consistent with prior work [60, 65, 103, 111, 117].

Hardware. We use systems with an AMD EPYC 9825 Processor, local DDR5-5600 memory, 8 lanes of CXL, and a 100 Gbit Mellanox CZ5 NIC. These systems are connected to pre-production 2-ported PDs with $\times 8$ links. All systems are interconnected with a 100 Gbit Arista 7060X series switch.

RPCs. For simplicity, we assume that RPCs requests have to reach a core, and that the core immediately sends its response, without computation. We implement RDMA RPCs using the `ib_send_lat` tool [67].

7.2 Pod Scalability and Cost

Scaling compared to fully-connected topologies. Table 2 compares fully-connected (FC) and Octopus topologies for different PD port counts. As the PD port count (N) increases, the number of hosts, H , increases faster for Octopus than for FC. For example, for $N = 2$, Octopus achieves a 4.5× larger pod size, whereas for $N = 16$, Octopus achieves a 7.6× larger pod size.

Note that these comparisons are assuming equal PD device costs. Specifically, the table assumes the same PD type for

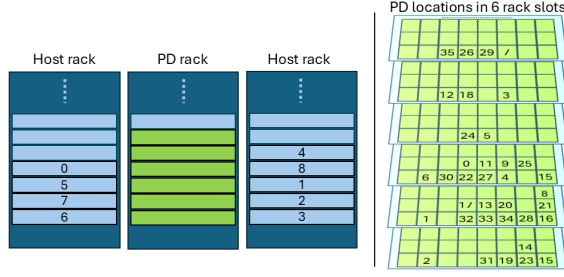


Figure 8. A 3-rack implementation of Octopus with 9 hosts and 36 2-port PDs, with corresponding logical topology shown in Figure 14. This layout requires 0.6 m cables. Logical host and device ids are shown in the slots they occupy.

PD ports (N)	CXL Pod Size (H)		Capex Cost iso. memory	Cable Len. Octopus
	FC	Octopus		
2	2	9	111%	0.6 m
4	4	25	113%	0.7 m
8	8	57	116%	1.1 m
16	16	121	125%	1.7 m

Table 2. Common CXL pod topologies for fully-connected (FC) and minimally-connected (Octopus) designs based on the assumption of $X = 8$ host ports. The capex is calculated as server costs with vs. without CXL, before accounting for memory savings through pooling. The cable length is the known minimum required to realize the Octopus topology within a 3-rack configuration.

both topologies and the number of PDs normalized by the number of hosts is the same. This reflects costs at hyperscale, where deployments span thousands of hosts.

Feasibility of physical layout. We attempt to solve the physical mapping SAT problem for various cable lengths to determine the length required to realize each topology in Table 3, as constructed using the cyclical construction algorithm in Appendix A. The cable lengths for which a solution was found within 3 hours of wall-clock time are documented in Table 3. Notably, 9- and 25-host topologies can be constructed using 0.7 m cables, which is feasible without retimers (Section 5.2). In contrast, 57- and 121-host topologies require <2 m cables, which likely requires retimers.

Sensitivity to the host port count X . Changes to the host port count, X , have no impact on the pod size for FC topologies. In contrast, Octopus linearly scales the pod size as a function of X . Thus, Octopus’s benefits materialize for $X > 1$.

Cost model sensitivity. Figure 9 assumes that for the 16-ported PD effective wafer costs and non-die costs are equal. We also evaluated costs assuming that wafer costs scale by $2\times$ and $\frac{1}{2}\times$, respectively. Generally, Octopus’s benefits remain

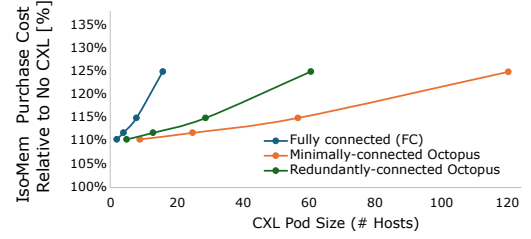


Figure 9. Fully-connected CXL pod topologies define a Pareto frontier where cost rises super-linearly with CXL pod size. For medium to large pod sizes, Octopus can achieve much larger pod sizes at equal or lower cost.

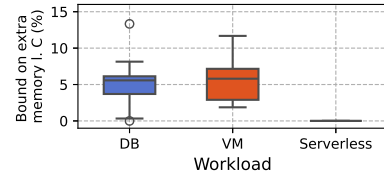


Figure 10. Additional memory required by Octopus relative to a FC design with the same host count for three production workloads. Note that a need for 5% more memory comparable favorably to enabling $4.5\times$ larger host counts (Table 2).

valid independent of these parameters. Appendix B includes figures showing these different cost models.

7.3 Dynamic Pod Memory Allocation

We evaluate our design using three production traces from multitenant platforms at Microsoft. Each trace contains tenant memory utilization over time, e.g., because of tenant VMs starting and stopping, or tenant databases requesting more memory. We calculate memory demand within each host and assign hosts into Octopus-25 pods. This results in 13 pods hosting databases, 18 pods hosting cloud VMs, and 69 pods hosting serverless workloads.

Analytic result. We use the traces to check the value of α suggested by the bound in Theorem 4.1 from Section 4. Our analysis focuses on the time of peak memory utilization in every pod. We then derive the value of α that fits the distribution of memory utilization across the hosts in each pod. Figure 10 shows the distribution of the resulting α values. In particular, the bound for database and cloud VM workloads are generally $<10\%$ of the memory required in a fully-connected pod, while serverless pods require no additional memory.

Simulation analysis. We complement our analytical results with a pooling simulation that covers all time steps in all three production traces. The simulation tracks the maximum memory used by all hosts and PDs in every pod.

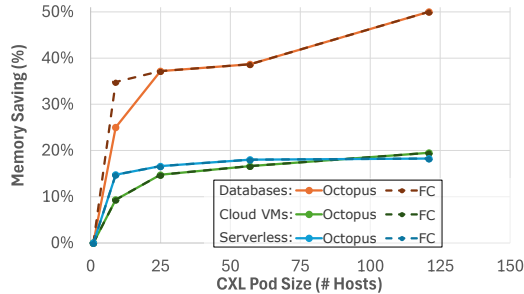


Figure 11. Pooling efficiency for three workloads, comparing Octopus to large (fictional) fully-connected topologies.

Figure 11 reports the resulting memory savings at different CXL pod sizes for FC and Octopus for the three traces. Note that we consider hypothetical FC pods with impractically large size (Table 1) to compare to Octopus as iso pod sizes.

We find significant memory savings in all three traces. Savings are increase steeply for 9 and 25 hosts, reach a plateau for 57 hosts and then increase again as we reach 121 hosts. Octopus matches the savings of FC almost perfectly, except for 9 hosts on the database trace. In this one instance, Octopus’s memory savings are 19% lower than FC’s savings.

Overall, Octopus’s memory allocation policy is highly effective for memory savings. Assuming that DRAM accounts for about half of overall server costs, Octopus achieves multiple configurations where CXL cost overheads are covered or almost covered by memory savings from dynamic memory allocation. For example, Octopus-25 has 3% lower Capex costs than a non-CXL system on database workloads, and reduces Capex overheads to 7% on VM and Serverless workloads. This means that CXL’s benefits for communication and other use cases may come at no additional cost for databases.

Hardware experiments. Prior work has shown techniques that enable datacenter workloads [60, 65, 76, 103, 111, 117] to mitigate performance impacts from added latency of CXL memory accesses. Specifically, the simulations assume that 50% of overall pod memory can come from PDs, with the other half remaining as local memory on hosts. Prior work has shown that this is feasible if CXL memory access latency is about 2× the local memory access latency. This is the case on today’s CXL systems [24]. In contrast, RDMA latencies are an order of magnitude higher and thus would not allow many workloads to use sufficient pool memory without performance slowdowns.

7.4 Pair-wise Communication and RPC Latency

As discussed in Section 2.2, the most common use case for CXL shared memory is pair-wise communication. Two common such use cases are microservice RPCs and key value store (KVS) APIs. Prior work has shown RPCs and KVS requests are small. For example, at Google, the majority of

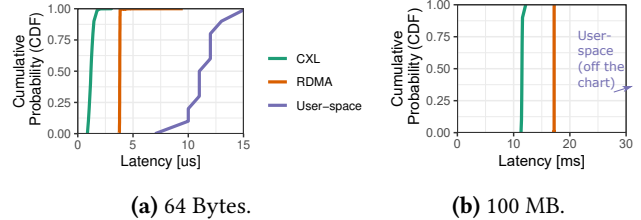


Figure 12. Distribution of RPC round-trip latency for small and large messages. CXL’s latency is 3.3× and 1.5× lower than RDMA, and 10× lower than user-space networking.

RPC services see median request sizes under 1500 Bytes with responses under 315 Bytes [94]. At Meta, almost all KVS request sizes fit into 128 Bytes and response sizes are typically around 1-10kB [15].

For small messages, a minimally-connected Octopus topology with H hosts has the same message-passing latency as a hypothetical FC topology with H hosts since every pair of hosts can directly exchange messages in both cases. Since Octopus matches FC, we compare CXL-based RPCs to RDMA and modern user-space networking [30] implementations. Figure 12a shows the round-trip latency distribution for these three RPC types for a message size of 64 bytes. The median latency of CXL RPCs is 1.2 μ s. RDMA RPCs are about 3.3× higher at 3.8 μ s and user-space networking is 9.5× higher at over 11 μ s. For the other end of the spectrum, Figure 12b shows round-trip latencies for 100MB RPCs. CXL remains 1.5× faster than RDMA even on these larger RPCs.

7.5 Pod-wide Distributed Shuffle

Distributed shuffle is a common use case for CXL pods (Section 2). Shuffle performance is influenced by multiple key parameters, including the number of participating hosts and the data skewness. Generally, as the number of participating hosts increases, each host needs to receive more data from others to aggregate the results. This makes comparing Octopus to FC difficult. In principle, Octopus should match the FC completion time, given the same number of hosts. However, Octopus topologies with more hosts than FC topologies have higher shuffle completion time.

We measure the completion time of a 64 GB uniform shuffle on our hardware. We compare a FC topology with an Octopus topology with the same $N = 2$ -ported PDs and $X = 2$ ports per host. The FC topology has $H = 2$ hosts, while the Octopus topology has $H = 3$ hosts. The analytical results show that the completion time is 33.6% higher with the Octopus topology. Given a 50% higher host cost, this tradeoff can make sense for compute-bound shuffles where adding hosts reduces overall completion time.

7.6 Pod-wide Broadcast

Broadcast benefits from FC pods where data is only written once and all hosts can access concurrently. In a minimally-connected Octopus topology, the broadcaster copies its data to all of its X PDs. Thus, Octopus broadcasts are slower than FC broadcasts by a factor of X , assuming the same pod size.

We use our hardware prototype to confirm this tradeoff for a 64 GB broadcast using a $N = 2$ -ported PDs and $X = 2$ ports per host. The FC topology has two hosts, while the Octopus topology has three hosts. From above’s analysis, we expect a $2\times$ slowdown for Octopus and we indeed measure a $1.98\times$ higher completion time. Thus, broadcast cast use cases may prefer a FC topology.

8 Discussion

Cost of specialization. Octopus topologies can be seen as optimizing for a subset of CXL pooling and sharing use cases, namely dynamic memory and pair-wise communication use cases. Octopus topologies are less optimal for sharing memory across the entire pool, requiring at best significant modifications to software prototypes (e.g., All-Gather [1]) and at worst limiting the benefits from sharing memory. We believe this is a useful tradeoff to get CXL pods widely deployed. Broad deployment may in turn reduce the premium of high-port-count PDs and switches, paving the way to fully-connected and switched topologies.

Support for fault tolerance and fail-in-place. A minimally-connected Octopus topology only offers a single path between any pair of hosts. If any CXL link or any PD fails, pod communication and many use cases will be severely affected. Redundantly-connected Octopus topologies overcome this challenge by offering λ redundant paths between any pair of hosts. It is rare for multiple failures to occur simultaneously [72]; we thus believe that low redundancy, e.g., $\lambda = 2$, strikes a useful balance between cost and redundancy.

Why dedicated CXL pooling devices? One might wonder why we focus on dedicated CXL devices if we consider pair-wise communication between hosts. One may use CXL to directly connect hosts or expose some host memory over CXL [3]. The practical reason is that dedicated CXL devices such as PDs are available today, whereas host-to-host CXL is not implemented today. Additionally, we’ve found that common CPU SoC fabrics poorly support cross-traffic arising from remote accesses, leading to high latency for local memory accesses. We also observe that a key deployment incentive for CXL is to add more or different memory to hosts [3, 106], which is not possible with host-to-host CXL.

Cabling Complexity and Management. Cable design, management, and connectors pose significant ongoing challenges in CXL pod deployments [9]. Compared to traditional systems with equivalent host and PD port counts, Octopus

topologies maintain or even reduce overall cabling complexity. Each host still requires the same number of outgoing CXL cables, but replacing a large PD with multiple smaller PDs reduces individual PD cable density, improving manageability and physical flexibility. However, scaling up pod sizes using Octopus topologies inherently introduces additional complexity due to increased cable counts and potentially intricate routing patterns. Industry-wide standardization and advances in connector technologies could significantly mitigate these challenges, simplifying the deployment, management, and scalability of large-scale CXL infrastructures.

Odd Numbers of Hosts per Pod. Octopus topologies inherently lead to pod configurations with odd numbers of hosts (Section 5.1). While this might initially appear counter-intuitive, e.g., with an expectation of familiar powers-of-two increments, it aligns well with practical constraints observed in modern data centers. In reality, racks are frequently only partially populated due to factors such as power distribution limits, cooling capabilities, and physical weight constraints. Consequently, deployments with non-power-of-two host counts are already prevalent in industry practice today.

Denser rack designs. Octopus conservatively assumes traditional air-cooled rack designs. Such racks typically use only a few dozen kW which limits the number of compute servers and CPUs [27]. Recent designs point to much higher rack power, e.g., above 100 kW [39, 88, 92]. Additionally, recent improvements in cooling technology enable server designs that require much less volume [53]. Combining high rack power with dense server designs can lead to hundreds of compute units becoming accessible within the reach of copper cabling. This would unlock even larger CXL pods where Octopus can excel at keeping latency and cost low.

Sparser CXL pod topologies. In addition to denser designs, Octopus can also scale with advanced topologies that are codesigned with applications. We call such topologies *sparse* as they do not require that pairs of hosts interconnect in a PD. Such sparse topologies may be especially useful in high-performance computing [7, 93]. For example, even small PDs allow constructing a high dimensional torus topology as used, e.g., in the Fugaku supercomputer [29, 31]. Another direction may be to draw inspiration from BCube [34] which may allow scaling to thousands of hosts, while minimizing latency and cost.

Limitations of our cost model. We believe that our current cost model significantly overestimates the cost of small PDs as it is difficult to account for their much higher volume. On the other hand, our cost comparison ignores chiplet-based PD designs that can alleviate IO pad constraints. This may benefit the cost of large PDs. However, chiplets come with significantly higher complexity, higher power consumption, and higher latency. Thus, PDs retain unique advantages even compared to chiplet-based designs. We finally remind

readers that all these numbers are for illustration purposes of the impact of CXL topologies on price and should not be interpreted otherwise.

9 Related Work

To the best of our knowledge, Octopus is the first work to compare different CXL pod topologies and physical layouts. Current state-of-practice follows either switch-based designs or fully-connected (FC) topologies with PDs. Prior work has shown that PDs with FC topologies are overall cheaper and faster than switches (Section 3). We explicitly compare FC and Octopus designs (Section 7).

Beyond CXL pooling, network and interconnection topologies have been studied extensively over several decades. In this context, PD-based topologies are known as point-to-point topologies [12] and have been superseded by switch-based designs [12, 23]. Historically, Ethernet networks have gone through multiple evolutionary phases starting with low-radix switches that lead to similar tradeoffs to small-port-count PDs (e.g., $N < 64$). This led to k-ary n-cubes [23] and tree topologies [61]. Tree topologies are similar to CXL 2.0 [48] switched topologies. Improvements in ASIC bandwidth enabled high-radix switches [51, 52]. High-radix switches and optical cabling then enabled modern Clos network topologies, as proposed in CXL 3.0 [80], and advanced low-diameter topologies [10, 13, 50, 51, 55]. CXL network topologies may undergo similar evolution as PCIe bandwidth further increases and eventually adopts optical cabling.

BCube [34] is a scalable topology for modular datacenters that uses low-port-count switches and relies on servers for routing. Similar to Octopus’s PDs, switches do not connect to other switches. A key difference, however, is that Octopus requires all servers to share at least one PD, while BCube can have paths as long as the number of ports in a server. Further, BCube is targeted at container-scale DCs, and its recursive nature implies that the highest-level cables be much longer than what is feasible with CXL.

Recent work has proposed custom network topologies for AllGather operations in distributed GPU AI training clusters, e.g., direct-connect fabrics [109] and rail-only topologies [108]. Overall, all these existing topologies are different from Octopus because they focus on connecting compute units with each other, instead of connecting compute units with memory pools.

10 Conclusion

Octopus challenges the prevailing assumption that effective CXL pods must employ fully-connected topologies with large pooling devices. Our minimally-connected topologies are cost-efficient and work well for major use cases such as dynamic memory allocation (resource pooling) and pair-wise communication. We formally prove and empirically show

that Octopus matches memory savings from pooling of a fully-connected topology, at much lower pod cost.

Octopus’s approach does involve trade-offs for specific use cases such as broadcast communication primitives. We believe that the overall benefits outweigh these tradeoffs for memory-intensive cloud and database workloads. Ultimately, Octopus offers a promising blueprint for CXL memory pooling infrastructures, balancing cost-effectiveness, scalability, and performance.

11 Acknowledgements

We would like to thank Midhul Vuppapapati for his valuable theoretical insights, which enabled the optimality analysis of Octopus dynamic memory allocations in Theorem 4.1. We are also grateful to Ricardo Bianchini and Rajesh Sankaran for their support and suggestions that helped improve the clarity of Octopus’s vision.

References

- [1] Hooyoung Ahn, Seonyoung Kim, Yoomi Park, Woojong Han, Shinyoung Ahn, Tu Tran, Bharath Ramesh, Hari Subramoni, and Dhaleswar K Panda. Mpi allgather utilizing cxl shared memory pool in multi-node computing systems. In *2024 IEEE International Conference on Big Data (BigData)*, pages 332–337. IEEE, 2024.
- [2] Minseon Ahn, Thomas Willhalm, Norman May, Donghun Lee, Suprasad Mutalik Desai, Daniel Booss, Jungmin Kim, Navneet Singh, Daniel Ritter, and Oliver Rebbholz. An examination of cxl memory use cases for in-memory database management systems using sap hana. *Proceedings of the VLDB Endowment*, 17(12):3827–3840, 2024.
- [3] Emmanuel Amaro, Stephanie Wang, Aurojit Panda, and Marcos K Aguilera. Logical memory pools: Flexible and local disaggregated memory. In *Proceedings of the 22nd ACM Workshop on Hot Topics in Networks*, pages 25–32, 2023.
- [4] AMD. AMD EPYC 9124 Specifications. <https://www.techpowerup.com/cpu-specs/epyc-9124.c2917>. Accessed: 2025-01-15.
- [5] Inc. Astera Labs. Aries pcie®/cxl® smart cable modules™. <https://www.asteralabs.com/products/aries-smart-cable-modules/>, 2024. Product Brief.
- [6] David F Bacon, Carsten Binnig, David Patterson, and Margo Seltzer. Hardware support for cloud database systems in the post-moore’s law era (dagstuhl seminar 24162). *Dagstuhl Reports*, 14(4):54–84, 2024.
- [7] Michael Barnett, Rick Littlefield, David G Payne, and Robert van de Geijn. Global combine on mesh architectures with wormhole routing. In *[1993] Proceedings Seventh International Parallel Processing Symposium*, pages 156–162. IEEE, 1993.
- [8] Alexander Baumstark, Marcus Paradies, Kai-Uwe Sattler, Steffen Kläbe, and Stephan Baumann. So far and yet so near-accelerating distributed joins with cxl. In *Proceedings of the 20th International Workshop on Data Management on New Hardware*, pages 1–9, 2024.
- [9] Daniel S Berger, Daniel Ernst, Huaicheng Li, Pantea Zardoshti, Monish Shah, Samir Rajadnya, Scott Lee, Lisa Hsu, Ishwar Agarwal, Mark D Hill, et al. Design tradeoffs in cxl-based memory pools for public cloud platforms. *IEEE Micro*, 43(2):30–38, 2023.
- [10] Maciej Besta and Torsten Hoefler. Slim fly: A cost effective low-diameter network topology. In *SC’14: proceedings of the international conference for high performance computing, networking, storage and analysis*, pages 348–359. IEEE, 2014.
- [11] Thomas Beth, Dieter Jungnickel, and Hanfried Lenz. *Design Theory*, volume 1. Cambridge University Press, Cambridge, UK, 2nd edition, 1999. Covers constructions of combinatorial designs, including BIBDs

- using finite projective planes.
- [12] Tobias Bjerregaard and Shankar Mahadevan. A survey of research and practices of network-on-chip. *ACM Computing Surveys (CSUR)*, 38(1):1–es, 2006.
- [13] Nils Blach, Maciej Besta, Daniele De Sensi, Jens Domke, Hussein Harake, Shigang Li, Patrick Iff, Marek Konieczny, Kartik Lakhotia, Ales Kubicek, et al. A {High-Performance} design, implementation, deployment, and evaluation of the slim fly network. In *21st USENIX Symposium on Networked Systems Design and Implementation (NSDI 24)*, pages 1025–1044, 2024.
- [14] R. C. Bose. On balanced incomplete block designs. *Annals of Human Genetics*, 9:353–399, 1939.
- [15] Zhichao Cao, Siying Dong, Sagar Vemuri, and David HC Du. Characterizing, modeling, and benchmarking {RocksDB} {Key-Value} workloads at facebook. In *18th USENIX Conference on File and Storage Technologies (FAST 20)*, pages 209–223, 2020.
- [16] Prakash Chauhan, Chris Petersen, Brian Morris, and Jerome Glisse. Hyperscale tiered memory expander specification for compute express link. Available at <https://www.opencompute.org/documents/hyperscale-tiered-memory-expander-specification-for-compute-express-link-cxl-1-pdf>, 2023. Open Compute Project, Revision 1, Effective October 27, 2023.
- [17] Lyndon Clarke, Ian Glendinning, and Rolf Hempel. The mpi message passing interface standard. In *Programming Environments for Massively Parallel Distributed Systems: Working Conference of the IFIP WG 10.3, April 25–29, 1994*, pages 213–218. Springer, 1994.
- [18] Daniel Cohen, Sarel Cohen, Dalit Naor, Daniel Waddington, and Moshik Hershcovitch. Dictionary based cache line compression. In *Proceedings of the 16th ACM Workshop on Hot Topics in Storage and File Systems*, pages 8–14, 2024.
- [19] Charles J. Colbourn and Jeffrey H. Dinitz, editors. *Handbook of Combinatorial Designs*. Chapman and Hall/CRC, 2nd edition, 2006.
- [20] Compute Express Link Consortium. Compute Express Link (CXL) Specification, Revision 2.0, November 2020. Accessed: 2025-03-11.
- [21] DG Corneil and RA MATHON. Algorithmic techniques for the generation and analysis of strongly regular graphs and other combinatorial configurations. In *Annals of Discrete Mathematics*, volume 2, pages 1–32. Elsevier, 1978.
- [22] Meghan Cowan, Saeed Maleki, Madanlal Musuvathi, Olli Saarikivi, and Yifan Xiong. Mscclang: Microsoft collective communication language. In *Proceedings of the 28th ACM International Conference on Architectural Support for Programming Languages and Operating Systems, Volume 2*, pages 502–514, 2023.
- [23] William J. Dally. Performance analysis of k-ary n-cube interconnection networks. *IEEE transactions on Computers*, 39(6):775–785, 1990.
- [24] Debendra Das Sharma, Robert Blankenship, and Daniel Berger. An introduction to the compute express link (cxl) interconnect. *ACM Computing Surveys*, 56(11):1–37, 2024.
- [25] Mohamad El-Batal. Seagate Composable Memory Appliance (CMA) Architecture. <https://www.youtube.com/watch?v=KCgE0WejXl0>, June 2024.
- [26] Mohammad Ewaes and Paul Chow. Disaggregated memory in the datacenter: A survey. *IEEE Access*, 11:20688–20712, 2023.
- [27] Xiaobo Fan, Wolf-Dietrich Weber, and Luiz Andre Barroso. Power provisioning for a warehouse-sized computer. *ACM SIGARCH computer architecture news*, 35(2):13–23, 2007.
- [28] R. A. Fisher and F. Yates. The construction of balanced incomplete block designs. *Annals of Human Genetics*, 9:30–43, 1938.
- [29] Riken Center for Computational Science. Fugaku: Japan’s super-computer successor to the k computer. *Riken Press Release*, 2020. Fugaku employs the Tofu interconnect, maintaining a 6D mesh/torus topology for scalability and performance.
- [30] Joshua Fried, Gohar Irfan Chaudhry, Enrique Saurez, Esha Choukse, Íñigo Goiri, Sameh Elnikety, Rodrigo Fonseca, and Adam Belay. Making kernel bypass practical for the cloud with junction. In *21st USENIX Symposium on Networked Systems Design and Implementation (NSDI 24)*, pages 55–73, 2024.
- [31] Fujitsu and RIKEN. K computer: The world’s first 10-petaflop super-computer. *Fujitsu Technical Journal*, 2011. The K Computer uses the Tofu interconnect, a proprietary 6D mesh/torus network topology.
- [32] Ellis Giles and Peter Varman. Acid support for compute express link memory transactions. In *SC24-W: Workshops of the International Conference for High Performance Computing, Networking, Storage and Analysis*, pages 982–995. IEEE, 2024.
- [33] Juncheng Gu, Youngmoon Lee, Yiwen Zhang, Mosharaf Chowdhury, and Kang G Shin. Efficient memory disaggregation with infiniswap. In *14th USENIX Symposium on Networked Systems Design and Implementation (NSDI 17)*, pages 649–667, 2017.
- [34] Chuanxiong Guo, Guohan Lu, Dan Li, Haitao Wu, Xuan Zhang, Yunfeng Shi, Chen Tian, Yongguang Zhang, and Songwu Lu. Bcube: a high performance, server-centric network architecture for modular data centers. In *Proceedings of the ACM SIGCOMM 2009 Conference on Data Communication*, SIGCOMM ’09, page 63–74, New York, NY, USA, 2009. Association for Computing Machinery.
- [35] Yunyan Guo and Guoliang Li. A cxl-powered database system: Opportunities and challenges. In *2024 IEEE 40th International Conference on Data Engineering (ICDE)*, pages 5593–5604. IEEE, 2024.
- [36] Minh Ha, Junhee Ryu, Jungmin Choi, Kwangjin Ko, Sunwoong Kim, Sungwoo Hyun, Donguk Moon, Byungil Koh, Hokyoon Lee, Myoungseo Kim, et al. Dynamic capacity service for improving cxl pooled memory efficiency. *IEEE Micro*, 43(2):39–47, 2023.
- [37] Ori Hadary, Luke Marshall, Ishai Menache, Abhishek Pan, Esaias E Greeff, David Dion, Star Dorminey, Shailesh Joshi, Yang Chen, Mark Russinovich, et al. Protean: {VM} allocation service at scale. In *14th USENIX Symposium on Operating Systems Design and Implementation (OSDI 20)*, pages 845–861, 2020.
- [38] David Hawkins and Matt Bromage. Design Considerations for CXL Device Hardware Coherency (HDM-DB). <https://www.youtube.com/watch?v=2ktM7dPcmql>, 2024.
- [39] Ali Heydari. How generative ai and accelerated compute is creating the next generation liquid cooled data centers with focus on challenges, opportunities and the road ahead. In *2024 IEEE Intersociety Conference on Thermal and Thermomechanical Phenomena in Electronic Systems (ITHERM)*, Gaylord Rockies, CO, May 2024. Keynote presentation.
- [40] Tao Huang, Yonggui Liang, Shubao Yu, and Kexin Chen. Txcocklet: an innovative solution for efficient cross-node data transmission enabled by cxl-based shared memory. *CCF Transactions on High Performance Computing*, January 2025. Regular Paper, Published: 22 January 2025.
- [41] Yibo Huang, Newton Ni, Vijay Chidambaram, Emmett Witchel, and Dixin Tang. Pasha: An efficient, scalable database architecture for cxl pods. In *15th Annual Conference on Innovative Data Systems Research (CIDR ’25)*, Amsterdam, The Netherlands, 2025. The University of Texas at Austin. Published under the Creative Commons Attribution 4.0 International (CC-BY 4.0) license.
- [42] P. Hunt, M. Konar, F. P. Junqueira, and B. Reed. Zookeeper: Wait-free coordination for internet-scale systems. In *Proceedings of the USENIX Annual Technical Conference (ATC)*, pages 145–158. USENIX Association, 2010.
- [43] Ronen Hyatt. The quest for bandwidth and capacity: Memory edition, 2023. https://www.hpcuserforum.com/wp-content/uploads/2023/09/Ronen-Hyatt_UnifabriX_The-Quest-for-Bandwidth-and-Capacity-Memory-Edition_Sept-2023-HPC-UF.pdf.
- [44] Alexey Ignatiev, Zi Li Tan, and Christos Karamanos. Towards universally accessible SAT technology. In *SAT*, pages 4:1–4:11, 2024.
- [45] JP Jiang. CXL Switch for Scalable & Composable Memory Pooling/Sharing. FMS presentation available at <https://www.xconn->

- tech.com/products, 2024.
- [46] F. P. Junqueira, B. C. Reed, and M. Serafini. Zab: High-performance broadcast for primary-backup systems. In *Proceedings of the IEEE/IFIP International Conference on Dependable Systems and Networks (DSN)*, pages 245–256. IEEE Computer Society, 2011.
 - [47] Michael Kalodrich. New supermicro x14 systems, 2024. Accessed: 2024-12-18.
 - [48] Jim Kao. CXL 2.0 Switch for a Composable Memory System. https://computeexpresslink.org/wp-content/uploads/2024/09/Xconn_CXL-2.0-Switch-for-a-Composable-Memory-System_FMS-2024_FINAL.pdf, October 2024.
 - [49] Patrick Kennedy. Lenovo has a cxl memory monster with 128x 128gb ddr5 dimms, 2024. Accessed: 2024-12-18.
 - [50] John Kim, William J Dally, Steve Scott, and Dennis Abts. Technology-driven, highly-scalable dragonfly topology. *ACM SIGARCH Computer Architecture News*, 36(3):77–88, 2008.
 - [51] John Kim, William J Dally, and Dennis Abts. Flattened butterfly: a cost-efficient topology for high-radix networks. In *Proceedings of the 34th annual international symposium on Computer architecture*, pages 126–137, 2007.
 - [52] John Kim, William J Dally, Brian Towles, and Amit K Gupta. Microarchitecture of a high radix router. In *32nd International Symposium on Computer Architecture (ISCA’05)*, pages 420–431. IEEE, 2005.
 - [53] Milin Kodnongbua, Zachary Englhardt, Ricardo Bianchini, Rodrigo Fonseca, Alvin Lebeck, Daniel S Berger, Vikram Iyer, Fiodar Kazhamiaka, and Adriana Schulz. Dense server design for immersion cooling. *ACM Transactions on Graphics (TOG)*, 43(6):1–20, 2024.
 - [54] Astera Labs. Leo cxl smart memory controllers. Available at <https://www.asteralabs.com/products/leo-cxl-smart-memory-controllers/>, December 2023. Product Brief.
 - [55] Kartik Lakhota, Maciej Besta, Laura Monroe, Kelly Isham, Patrick Iff, Torsten Hoefler, and Fabrizio Petrini. Polarfly: a cost-effective and flexible low-diameter topology. In *SC22: International Conference for High Performance Computing, Networking, Storage and Analysis*, pages 1–15. IEEE, 2022.
 - [56] Leslie Lamport. The part-time parliament. *ACM Transactions on Computer Systems (TOCS)*, 16(2):133–169, May 1998.
 - [57] Richard Langlois and Edward Steinmueller. The evolution of competitive advantage in the worldwide semiconductor industry. *Sources of industrial leadership*. Cambridge University Press, Cambridge, UK, 1999.
 - [58] Donghun Lee, Thomas Willhalm, Minseon Ahn, Suprasad Muralik Desai, Daniel Booss, Navneet Singh, Daniel Ritter, Jungmin Kim, and Oliver Rebholz. Elastic use of far memory for in-memory database management systems. In *Proceedings of the 19th International Workshop on Data Management on New Hardware*, pages 35–43, 2023.
 - [59] Donghyuk Lee and Onur Mutlu. Dram scaling challenges and solutions. *IEEE Micro*, 42(2):14–25, 2022.
 - [60] Taehyung Lee, Sumit Kumar Monga, Changwoo Min, and Young Ik Eom. Memtis: Efficient memory tiering with dynamic page classification and page size determination. In *Proceedings of the 29th Symposium on Operating Systems Principles*, pages 17–34, 2023.
 - [61] Charles E Leiserson. Fat-trees: Universal networks for hardware-efficient supercomputing. *IEEE transactions on Computers*, 100(10):892–901, 1985.
 - [62] Lenovo. Lenovo thinksystem sr860 v3 server, 2024. Accessed: 2024-12-18.
 - [63] Alberto Lerner and Gustavo Alonso. Cxl and the return of scale-up database engines. *arXiv preprint arXiv:2401.01150*, 2024.
 - [64] Philip Levis, Kun Lin, and Amy Tai. A case against cxl memory pooling. In *Proceedings of the 22nd ACM Workshop on Hot Topics in Networks*, pages 18–24, 2023.
 - [65] Huaicheng Li, Daniel S. Berger, Lisa Hsu, Daniel Ernst, Pantea Zardoshti, Stanko Novakovic, Monish Shah, Samir Rajadnya, Scott Lee, Ishwar Agarwal, Mark D. Hill, Marcus Fontoura, and Ricardo Bianchini. Pond: CXL-Based Memory Pooling Systems for Cloud Platforms. In *ASPLOS*, 2023.
 - [66] Kevin Lim, Yoshio Turner, Jose Renato Santos, Alvin AuYoung, Jichuan Chang, Parthasarathy Ranganathan, and Thomas F Wenisch. System-level implications of disaggregated memory. In *IEEE International Symposium on High-Performance Comp Architecture*, pages 1–12. IEEE, 2012.
 - [67] linux rdma. Perftest: Infiniband verbs performance tests, 2025. Accessed: 2025-03-12.
 - [68] B. Liskov and J. Cowling. Viewstamped replication revisited. Technical Report MIT-CSAIL-TR-2012-021, MIT, July 2012.
 - [69] Brian Liskov and Robert Scheifler. The primary-backup approach to fault-tolerant distributed systems. In *Proceedings of the 7th ACM Symposium on Operating Systems Principles (SOSP)*, pages 48–55. ACM, 1979.
 - [70] Jinshu Liu, Hamid Hadian, Yuyue Wang, Daniel S. Berger, Marie Nguyen, Xun Jian, Sam H. Noh, and Huaicheng Li. Systematic CXL memory characterization and performance analysis at scale. In *Proceedings of the 2025 ACM International Conference on Architectural Support for Programming Languages and Operating Systems (ASPLOS’25)*, 2025.
 - [71] Nathan Luehr. Nvidia collective communications library (nccl). <https://developer.nvidia.com/nccl>, 2016. Accessed 1/1/2025.
 - [72] Jialun Lyu, Marisa You, Celine Irvine, Mark Jung, Tyler Narmore, Jacob Shapiro, Luke Marshall, Savyasachi Samal, Ioannis Manousakis, Lisa Hsu, et al. Hyrax: {Fail-in-Place} server operation in cloud platforms. In *17th USENIX Symposium on Operating Systems Design and Implementation (OSDI 23)*, pages 287–304, 2023.
 - [73] Teng Ma, Zheng Liu, Chengkun Wei, Jialiang Huang, Youwei Zhuo, Haoyu Li, Ning Zhang, Yijin Guan, Dimin Niu, Mingxing Zhang, et al. {HydraRPC}:: {RPC} in the {CXL} era. In *2024 USENIX Annual Technical Conference (USENIX ATC 24)*, pages 387–395, 2024.
 - [74] Grant Mackey. You don’t know ‘jack’: Cxl fabric orchestration and management. Available at https://files.futurememorystorage.com/proceedings/2024/20240806_CXLT-102-1_Mackey.pdf, 2024. Presented by Jackrabbit Labs.
 - [75] Suyash Mahar, Ehsan Hajyjasini, Seungjin Lee, Zifeng Zhang, Mingyao Shen, and Steven Swanson. Telepathic datacenters: Fast rpcs using shared cxl memory, 2024.
 - [76] Hasan Al Maruf, Hao Wang, Abhishek Dhanotia, Johannes Weiner, Niket Agarwal, Pallab Bhattacharya, Chris Petersen, Mosharaf Chowdhury, Shobhit Kanaujia, and Prakash Chauhan. Tpp: Transparent page placement for cxl-enabled tiered-memory. In *Proceedings of the 28th ACM International Conference on Architectural Support for Programming Languages and Operating Systems, Volume 3*, pages 742–755, 2023.
 - [77] Inc. Marvell Technology. Structera a 2504 memory-expansion controller. Available at <https://www.marvell.com/content/dam/marvell/en/public-collateral/assets/marvell-structera-a-2504-near-memory-accelerator-product-brief.pdf>, 2024. Product Brief, P/N MV-SLA25041-A0-HF350AA-C000.
 - [78] MemVerge. Memverge unveils world’s first cxl-based multi-server shared memory at isc. Press release, May 2023. International Supercomputing Conference (ISC), Hamburg, Germany.
 - [79] Michael Mitzenmacher. The power of two choices in randomized load balancing. *IEEE Transactions on Parallel and Distributed Systems*, 12(10):1094–1104, 2001.
 - [80] Danny Moore and Debendra Das Sharma. CXL 3.0: Enabling composable systems with expanded fabric capabilities. https://computeexpresslink.org/wp-content/uploads/2023/12/CXL_3.0-Webinar_FINAL.pdf, October 2022.
 - [81] Benjamin Munger, Kathy Wilcox, Jeshuah Sniderman, Chuck Tung, Brett Johnson, Russell Schreiber, Carson Henrion, Kevin Gillespie,

- Tom Burd, Harry Fair, David Johnson, Jonathan White, Scott McLeland, Steven Bakke, Javin Olson, Ryan McCracken, Matthew Pickett, Aaron Horiuchi, Hien Nguyen, and Tim H Jackson. "zen 4": The amd 5nm 5.7ghz x86-64 microprocessor core. In *2023 IEEE International Solid-State Circuits Conference (ISSCC)*, pages 38–39, 2023.
- [82] Onur Mutlu. Memory scaling: A systems architecture perspective. *International Memory Workshop (IMW)*, 2013.
- [83] Author Name. *Investigating States and Logged Contents in CXL Memory*. PhD thesis, University Name, 2025.
- [84] OCP NIC subgroup OCP Server Workgroup. *OCP NIC 3.0 Design Specification Version 1.5.0 - Release*, September 2024. Available at <https://drive.google.com/file/d/1z7MU6Lpu8xQ19rprxHrL1bjaxt106iV/view>.
- [85] Diego Ongaro and John Ousterhout. In search of an understandable consensus algorithm. In *2014 USENIX annual technical conference (USENIX ATC 14)*, pages 305–319, 2014.
- [86] Pitch Patarasuk and Xin Yuan. Bandwidth optimal all-reduce algorithms for clusters of workstations. *Journal of Parallel and Distributed Computing*, 69(2):117–124, 2009.
- [87] ASRock Rack. Gnr8-2l2t preliminary ceb specifications, 2024. Accessed: 2024-12-18.
- [88] Ramboll. 100+ kw per rack in data centers: The evolution and revolution of power density, 2023.
- [89] Matthias Ryser, Simon Leier, Andrej Vodisek, Gustavo Alonso, and Torsten Hoefler. Bringing zero-copy rdma to database systems. In *CIDR '22: Conference on Innovative Data Systems Research*, 2022.
- [90] Ariane Rüdiger. Unifabrix bringt Memory-Pooling-System auf den Markt. <https://www.storage-insider.de/unifabrix-bringt-memory-pooling-system-auf-den-markt-a-16174bc8ab4a68a83b44fca6a0fca3b0/>, June 2023.
- [91] Inc. Samtec. Successful pcie interconnect guidelines, 2021. Available at https://blog.samtec.com/wp-content/uploads/2021/04/04_15_2021_successful_PCIE_interconnect_guidelines.pdf. Accessed March 11, 2025.
- [92] Schneider Electric. The ai disruption: Challenges and guidance for data center design. Technical report, Schneider Electric Energy Management Research Center, 2023.
- [93] David S Scott. Efficient all-to-all communication patterns in hypercube and mesh topologies. In *The Sixth Distributed Memory Computing Conference, 1991. Proceedings*, pages 398–399. IEEE Computer Society, 1991.
- [94] Korakit Seemakhupt, Brent E Stephens, Samira Khan, Sihang Liu, Hassan Wassel, Soheil Hassas Yeganeh, Alex C Snoeren, Arvind Krishnamurthy, David E Culler, and Henry M Levy. A Cloud-Scale Characterization of Remote Procedure Calls. In *SOSP*, 2023.
- [95] Aashaka Shah, Vijay Chidambaram, Meghan Cowan, Saeed Maleki, Madan Musuvathi, Todd Mytkowicz, Jacob Nelson, Olli Saarikivi, and Rachee Singh. {TACCL}: Guiding collective algorithm synthesis using communication sketches. In *20th USENIX Symposium on Networked Systems Design and Implementation (NSDI 23)*, pages 593–612, 2023.
- [96] S. S. Shrikhande. A survey of balanced incomplete block designs. *Journal of Combinatorial Theory, Series A*, 15(3):271–291, 1973.
- [97] A. B. Smith and J. L. Walrand. Integrated circuit yield and cost analysis: A critical area approach. In *Proceedings of the IEEE International Conference on VLSI Design*, pages 115–120. IEEE, 2005.
- [98] Douglas R. Stinson. *Combinatorial Designs: Constructions and Analysis*. Springer, 2004.
- [99] KAYTUS Systems. Kr2280v3 platform intel amd, 2024. Accessed: 2024-12-18.
- [100] Steven Telian. Pcie gen5 signal integrity implementation. In *DesignCon 2023*, 2023. Available at https://siguys.com/wp-content/uploads/2023/02/DesCon23_PAPER_Track7_PCIEGen5SignalIntegrityImplementation_Telian.pdf. Accessed March 11, 2025.
- [101] Yong Tian. Project gismo: Global i/o-free shared memory objects. Presented at Flash Memory Summit (FMS) 2023, <https://memverge.com/wp-content/uploads/MemVerge-Gismo-FMS2023.pdf>, 2023.
- [102] Muhammad Tirmazi, Adam Barker, Nan Deng, Md E Haque, Zhi-jing Gene Qin, Steven Hand, Mor Harchol-Balter, and John Wilkes. Borg: the next generation. In *Proceedings of the fifteenth European conference on computer systems*, pages 1–14, 2020.
- [103] Midhul Vuppapapati and Rachit Agarwal. Tiered memory management: Access latency is the key! In *Proceedings of the ACM SIGOPS 30th Symposium on Operating Systems Principles*, pages 79–94, 2024.
- [104] Mahesh Wagh and Rick Sodke. Compute express link 2.0 specification: Memory pooling. Available at <https://computeexpresslink.org/wp-content/uploads/2023/12/CXL-2.0-Memory-Pooling.pdf>, 2021. Presented at the CXL Consortium.
- [105] Jacob Wahlgren, Maya Gokhale, and Ivy B Peng. Evaluating emerging cxl-enabled memory pooling for hpc systems. In *2022 IEEE/ACM Workshop on Memory Centric High Performance Computing (MCHPC)*, pages 11–20. IEEE, 2022.
- [106] Jaylen Wang, Daniel S Berger, Fiodar Kazhamiaka, Celine Irvine, Chaojie Zhang, Esha Choukse, Kali Frost, Rodrigo Fonseca, Brijesh Warriar, Chetan Bansal, et al. Designing cloud servers for lower carbon. In *2024 ACM/IEEE 51st Annual International Symposium on Computer Architecture (ISCA)*, pages 452–470. IEEE, 2024.
- [107] Jianguo Wang and Qizhen Zhang. Disaggregated database systems. In *Companion of the 2023 International Conference on Management of Data*, pages 37–44, 2023.
- [108] Weiyang Wang, Manya Ghobadi, Kayvon Shakeri, Ying Zhang, and Naader Hasani. Rail-only: A low-cost high-performance network for training llms with trillion parameters. In *2024 IEEE Symposium on High-Performance Interconnects (HOTI)*, pages 1–10. IEEE, 2024.
- [109] Weiyang Wang, Moein Khazraee, Zhizhen Zhong, Manya Ghobadi, Zhihao Jia, Dheevatsa Mudigere, Ying Zhang, and Anthony Kewitsch. {TopoOpt}: Co-optimizing network topology and parallelization strategy for distributed training jobs. In *20th USENIX Symposium on Networked Systems Design and Implementation (NSDI 23)*, pages 739–767, 2023.
- [110] XConn. XC50256 CXL 2.0 Switch Chip. <https://www.xconn-tech.com/products>, 2024.
- [111] Lingfeng Xiang, Zhen Lin, Weishu Deng, Hui Lu, Jia Rao, Yifan Yuan, and Ren Wang. Nomad: {Non-Exclusive} memory tiering via transactional page migration. In *18th USENIX Symposium on Operating Systems Design and Implementation (OSDI 24)*, pages 19–35, 2024.
- [112] Chuha Xu, Yiyu Liu, Zijun Li, Quan Chen, Han Zhao, Deze Zeng, Qian Peng, Xueqi Wu, Haifeng Zhao, Senbo Fu, et al. Faasmem: Improving memory efficiency of serverless computing with memory pool architecture. In *Proceedings of the 29th ACM International Conference on Architectural Support for Programming Languages and Operating Systems, Volume 3*, pages 331–348, 2024.
- [113] Maofan Yin, Dahlia Malkhi, Michael K Reiter, Guy Golan Gueta, and Ittai Abraham. Hotstuff: Bft consensus with linearity and responsiveness. In *Proceedings of the 2019 ACM Symposium on Principles of Distributed Computing*, pages 347–356, 2019.
- [114] Irene Zhang, Zain R. Asgar, Sourav Kundu, and Anuj Kalia. Cornflakes: Zero-copy serialization for microsecond-scale datacenter services. In *SOSP '23: ACM Symposium on Operating Systems Principles*, 2023.
- [115] Jie Zhang, Xuzheng Chen, Yin Zhang, and Zeke Wang. Dmrpc: Disaggregated memory-aware datacenter rpc for data-intensive applications. In *2024 IEEE 40th International Conference on Data Engineering (ICDE)*, pages 3796–3809. IEEE, 2024.
- [116] Mingxing Zhang, Teng Ma, Jinqi Hua, Zheng Liu, Kang Chen, Ning Ding, Fan Du, Jinlei Jiang, Tao Ma, and Yongwei Wu. Partial failure resilient memory management system for (cxl-based) distributed

- shared memory. In *Proceedings of the 29th Symposium on Operating Systems Principles*, SOSP '23, page 658–674, New York, NY, USA, 2023. Association for Computing Machinery.
- [117] Yuhong Zhong, Daniel S Berger, Carl Waldspurger, Ryan Wee, Ishwar Agarwal, Rajat Agarwal, Frank Hady, Karthik Kumar, Mark D Hill, Mosharaf Chowdhury, et al. Managing memory tiers with {CXL} in virtualized environments. In *18th USENIX Symposium on Operating Systems Design and Implementation (OSDI 24)*, pages 37–56, 2024.
- [118] Yuhong Zhong, Daniel S. Berger, Pantea Zardoshti, Enrique Saurez, Jacob Nelson, Antonis Psistakis, Joshua Fried, and Asaf Cidon. Beware, pcie switches! cxl pools are out to get you. In *Proceedings of the 20th Workshop on Hot Topics in Operating Systems (HotOS XX)*, Banff, Alberta, Canada, May 2025. ACM SIGOPS.
- [119] Zhiting Zhu, Newton Ni, Yibo Huang, Yan Sun, Zhipeng Jia, Nam Sung Kim, and Emmett Witchel. Lupin: Tolerating partial failures in a cxl pod. In *Proceedings of the 2nd Workshop on Disruptive Memory Systems*, pages 41–50, 2024.

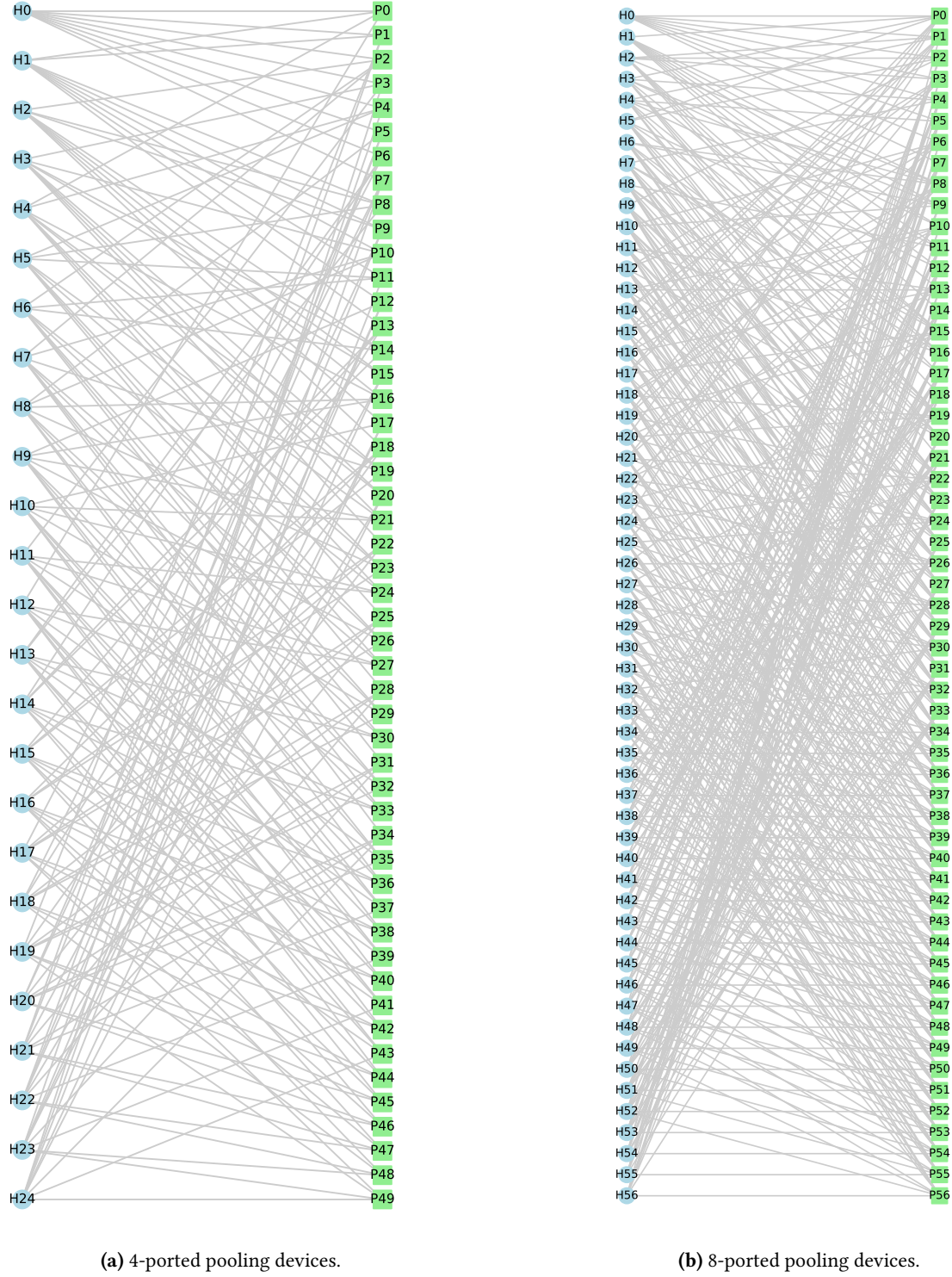


Figure 13. Minimally-connected Octopus topologies for the common case of $X = 8$ host ports. (a) visualizes design #2 in Table 3 with $N = 4$ -ported PDs. This design spans $H = 25$ hosts. (b) visualizes design #3 in Table 3 with $N = 8$ -ported PDs. This design spans $H = 57$ hosts.

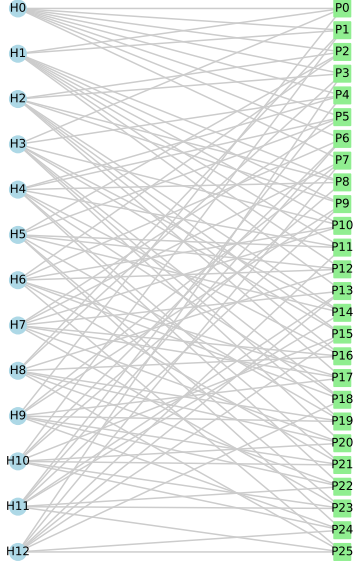


Figure 15. Redundantly-connected Octopus topology for $N = 4$ -ported PDs and the common case of $X = 8$ host ports (design #6 in Table 4). The topology spans $H = 13$ hosts and offers two paths through common PDs between any pair of hosts.

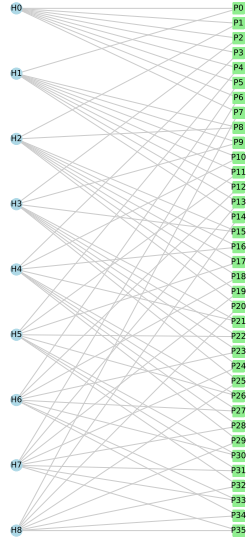


Figure 14. Minimally-connected Octopus topology for $N = 2$ -ported PDs and the common case of $X = 8$ host ports (design #1 in Table 3). The topology spans $H = 9$ hosts.

A Constructing Octopus Topologies

As discussed in Section 5, designing Octopus topologies is an equivalent mathematical problem to finding Balanced Incomplete Block Designs (BIBDs). BIBDs are combinatorial arrangements originally developed for designing statistical

experiments. Within BIBD, there are many different construction methods leading to different properties. In Octopus, we specifically want topologies that are not partitionable and highly symmetrical. These requirements lead to using cyclical construction methods, which are described in more detail below and well covered in existing mathematical literature [11, 19, 98].

We overview 12 particularly practical topologies in Tables 3, 4, 5. Specifically, Table 3 reviews four topologies already discussed and used in the evaluation, using $X = 8$ host CXL ports. Figure 13 visualizes two of these designs. Table 4 shows four smaller topologies using $X = 4$ host CXL ports. These eight topologies are minimally connected.

Table 5 shows redundantly-connected topologies, where any two hosts are connected to $\lambda = 2$ common PDs, again using $X = 8$ host CXL ports. One can think about redundantly-connected topologies as deriving two different $X = 4$ topologies and connecting each host to both, leading to an $X = 8$ topology with $\lambda = 2$. In fact, this is how they are commonly constructed in the literature. Figure 15 visualizes a small redundantly-connected topology with 4-ported PDs.

We show the general cyclical construction approach in Listing 1. To work with a topology, we find that incidence matrices, representing hosts as rows and pooling devices (PDs) as columns are most convenient. Thus, we provide code to reproduce these incidence matrices for all topologies discussed in Octopus. Listing 2 shows how to construct the four $X = 8$ topologies using this approach, Listing 3 shows $X = 4$, and Listing 4 shows $\lambda = 2$ and $X = 4$.

The next two subsections formalize the relationship of Octopus topologies to BIBD theory.

A.1 Equivalence to Balanced Incomplete Block Designs

We formally prove the equivalence between Octopus topologies and BIBDs. A BIBD is defined by parameters (v, b, r, k, λ) , where:

1. v : number of treatments (hosts),
2. b : number of blocks (PDs),
3. r : blocks per treatment (PDs per host),
4. k : treatments per block (hosts per PD),
5. λ : blocks containing each pair of treatments.

A minimally-connected Octopus topology corresponds to a BIBD with $\lambda = 1$. Given the constraints in Octopus topology:

- Every host (treatment) connects to exactly X PDs (blocks), thus $r = X$.
- Every PD connects exactly to N hosts, thus $k = N$.
- Any two distinct hosts connect through exactly one common PD, thus $\lambda = 1$.

These constraints match precisely the defining properties of a BIBD. Classical BIBD theory yields the relationships:[14, 28, 96]

$$b \times k = v \times r$$

$$r \times (k - 1) = \lambda \times (v - 1)$$

Substituting $\lambda = 1$, we recover:

$$H = v = 1 + X \times (N - 1), \quad M = b = \frac{H \times X}{N}.$$

This confirms that minimally-connected Octopus topologies are equivalent to BIBDs with $\lambda = 1$.

A.2 Cyclical Construction Methods

Although constructing general BIBDs is NP-hard, cyclical methods simplify the construction for specific parameter sets useful in Octopus topologies. A cyclical construction method arranges elements cyclically, generating blocks via systematic cyclic shifts. Specifically, let H hosts be numbered from 0 to $H - 1$. Given parameters X and N , define an initial block (PD) as an arithmetic progression modulo H . The remaining blocks result from cyclically shifting the initial block by increments:

$$B_0 = \{0, d, 2d, \dots, (N - 1)d\} \mod H,$$

where d is relatively prime to H . Subsequent blocks are:

$$B_i = (B_0 + i) \mod H, \quad \text{for } i = 1, 2, \dots, M - 1.$$

The cyclical structure provides symmetry, significantly simplifying the design and verification of Octopus topologies.

```

1 def develop_design(v, base_blocks):
2     """
3     Given a cyclic group of order v and a list of
4     base blocks, each of which may be:
5     - a list of integers (to be developed
6     fully), or
7     - a tuple (block, shifts) where 'shifts' is
8     an iterable of prescribed shifts,
9     return the full design by developing each
10    base block modulo v.
11    """
12    design = []
13    for B in base_blocks:
14        # If B is a tuple, unpack it; otherwise,
15        # use all shifts (0,...,v-1)
16        if isinstance(B, tuple):
17            block, shifts = B
18        else:
19            block, shifts = B, range(v)
20        for shift in shifts:
21            developed = sorted(((x + shift) % v)
22                               for x in block)
23            design.append(developed)
24    design.sort()
25    return design
26
27 def incidence_matrix(v, design):
28     """
29     Construct the incidence matrix for a design
30     on v points.
31     Rows correspond to points 0,...,v-1 and
32     columns to blocks.
33     """
34    b = len(design)
35    matrix = [[0] * b for _ in range(v)]
36    for j, block in enumerate(design):

```

```

29     for pt in block:
30         matrix[pt][j] = 1
31     return matrix

```

Listing 1. Octopus Topology Construction

```

1 # Acadia #1: 2-(9,2,1)
2 base_blocks_9 = [
3     ([0, 1]), ([0, 3]), ([0, 4]), ([0, 7])
4 ]
5 design_9 = develop_design(9, base_blocks_9)
6 incidence_9 = incidence_matrix(9, design_9)
7
8 # Acadia #2: 2-(25,4,1)
9 base_blocks_25 = [
10     ([0, 2, 6, 7]),
11     ([0, 1, 4, 12])]
12 design_25 = develop_design(25, base_blocks_25)
13 incidence_25 = incidence_matrix(25, design_25)
14
15 # Acadia #3: 2-(57,8,1)
16 base_blocks_57 = [
17     ([0, 1, 3, 5, 15, 17, 20, 24])]
18 design_57 = develop_design(57, base_blocks_57)
19 incidence_57 = incidence_matrix(57, design_57)
20
21 # Acadia #4: 2-(121,16,1)
22 B1_121 = ([0, 1, 3, 9, 10, 13, 27, 28, 30, 31,
23           36, 42, 55, 60, 68, 76])
24 B2_121 = ([0, 1, 3, 9, 10, 13, 27, 28], range(11))
25 design_121 = develop_design(121, [B1_121, B2_121])
26 incidence_121 = incidence_matrix(121, design_121)

```

Listing 2. $\lambda = 1$ Topologies for $X = 8$

```

1 # Acadia #5: 2-(5,2,1)
2 base_blocks_5 = [
3     ([0, 1]),
4     ([0, 2])]
5 design_5 = develop_design(5, base_blocks_5)
6 incidence_5 = incidence_matrix(5, design_5)
7
8 # Acadia #6: 2-(13,4,1)
9 base_blocks_13 = [
10     ([0, 1, 3, 9])]
11 design_13 = develop_design(13, base_blocks_13)
12 incidence_13 = incidence_matrix(13, design_13)
13
14 # Acadia #7: 2-(29,8,1)
15 B1_29 = ([0, 1, 4, 6, 10, 13, 17, 20], range(14))
16 B2_29 = ([0, 1, 4, 6], range(1)) # short orbit:
17     1 shift only
18 design_29 = develop_design(29, [B1_29, B2_29])
19 incidence_29 = incidence_matrix(29, design_29)
20
21 # Acadia #8: 2-(61,16,1)
22 B1_61 = ([0, 1, 3, 9, 10, 13, 20, 22, 25, 30, 35,
23           40, 45, 50, 55, 60])
24 B2_61 = ([1, 11, 60, 50], range(15)) #
25     quarter-filled PD
26 design_61 = develop_design(61, [B1_61, B2_61])
27 incidence_61 = incidence_matrix(61, design_61)

```

Listing 3. $\lambda = 1$ Topologies for $X = 4$

#	PD ports (N)	CXL pod size (H)	PD count (M)	Server Cost	PD Cost (\$ / host)	BIBD Model
1	2	9	36	111%	1120	2-(9,2,1)
2	4	25	50	113%	1280	2-(25,4,1)
3	8	57	57	116%	1620	2-(57,8,1)
4	16	121	60.5	125%	2493	2-(121,16,1)

Table 3. Octopus pod designs for the common case of $X = 8$ host CXL ports. These are the same configurations as shown in Table 2.

#	PD ports (N)	CXL pod size (H)	PD count (M)	Server Cost	PD Cost (\$ / host)	BIBD Model
5	2	5	10	106%	560	2-(5,2,1)
6	4	13	13	106%	640	2-(13,4,1)
7	8	29	14.5	108%	810	2-(29,8,1)
8	16	61	15.25	112%	1240	2-(61,16,1)

Table 4. Small Octopus pod designs based on $X = 4$ host CXL ports.

#	PD ports (N)	CXL pod size (H)	PD count (M)	Server Cost	PD Cost (\$ / host)	BIBD Model
9	2	5	20	111%	1120	2-(5,2,2)
10	4	13	26	113%	1280	2-(13,4,2)
11	8	29	29	116%	1620	2-(29,8,2)
12	16	61	30.5	125%	2500	2-(61,16,2)

Table 5. Redundantly-connected Octopus pod designs ($\lambda = 2$) for $X = 8$ host CXL ports.

```

1 # Acadia #9: 2-(5,2,2)
2 base_blocks_5_lambda2 = [
3     ([0, 1]), ([0, 1]), ([0, 2]), ([0, 2])]
4 design_5_lambda2 = develop_design(5,
5     base_blocks_5_lambda2)
6 incidence_5_lambda2 = incidence_matrix(5,
7     design_5_lambda2)
8
9 # Acadia #10: 2-(13,4,2)
10 base_blocks_13_lambda2 = [
11     ([0, 1, 3, 9]), ([0, 2, 5, 6])]
12 design_13_lambda2 = develop_design(13,
13     base_blocks_13_lambda2)
14 incidence_13_lambda2 = incidence_matrix(13,
15     design_13_lambda2)
16
17 # Acadia #11: 2-(29,8,2)
18 base_blocks_29_lambda2 = [
19     ([0, 1, 4, 6, 13, 16, 21, 25])]
20 design_29_lambda2 = develop_design(29,
21     base_blocks_29_lambda2)
22 incidence_29_lambda2 = incidence_matrix(29,
23     design_29_lambda2)
24
25 # Acadia #12: 2-(61,16,2)
26 B1_61_2 = ([0, 1, 3, 9, 10, 13, 20, 22, 25, 30,
27     35, 40, 45, 50, 55, 60], range(30))

```

```

22 B2_61_2 = ([0, 1, 3, 9, 10, 13, 27, 28], range(1))
23 design_61_2 = develop_design(61, [B1_61_2,
24     B2_61_2])
25 incidence_61_2 = incidence_matrix(61, design_61_2)

```

Listing 4. $\lambda = 2$ Topologies for $X = 8$

B Cost Model Assumptions and Sensitivity Study

We model PDs that use $N = 2, 4, 8, 16$ CXL ports with each port using $\times 8$ lanes. We scale the number of DDR5 somewhat proportionally to N , which matches existing designs at both ends of the parameter space.

We base our estimates on a PD die area model for a 5nm design proposed by ARM [38] and the 6nm design of the AMD Zen4 (Genoa) IO Die [81]. The ARM design assumes eight $\times 8$ CXL ports ($N = 8$) and 8 DDR5 channels. The assumption of $N = 8$ is common in existing proposals for large PDs [25, 36, 65, 74, 104]. We use the AMD IO die to estimate die area for an even larger PD with $N = 16$. Such large PDs have also been proposed by multiple companies [65, 90].

We downscale the ARM die area model to include smaller PDs with $N = 2$ and $N = 4$ ports. We remark that, while $N = 2$ is common for small PDs today, industry trends point

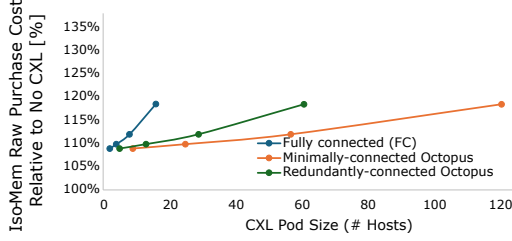


Figure 16. Assuming that wafers cost half as much as in Figure 9 compresses the overall cost differences. Octopus’s benefits remain similar.

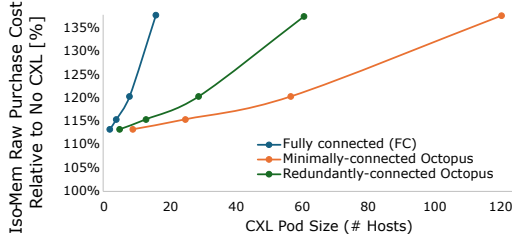


Figure 17. Assuming that wafers cost twice as much as in Figure 9 compresses the overall cost differences. Octopus’s benefits remain similar.

towards $N = 4$ devices for CXL 3.0/PCIe 6 by offering $\times 4$ CXL lanes per port at equal bandwidth to $\times 8$ lanes in PCIe5.

Our die area estimates scales super linearly with N , e.g., $N = 8$ and $N = 16$ require $5\times$ and $13\times$ the die area of $N = 2$ at only $4\times$ and $8\times$ the port count, respectively. The super-linear increase is due to the large number of IO pads required for the CXL and DDR5 ports, which has been widely discussed in the industry CXL community [38]. There are proposals to exploit the IO limitation to colocate other functionality on the PD. However, the ROI of that approach unclear, whereas we have a better understanding of the value and ROI of memory pooling [9].

We translate the die area estimates into relative cost estimates by assuming a standard 300mm wafer and a cost model based on critical die area yield and non-die costs [97]. Wafer costs are assumed to be discounted based on production volumes, assuming that smaller PDs are going to be a higher-volume product [57]. We remark that small $N = 2$ PDs are the only CXL PD with volume product today. To parameterize the cost model, we set the cost of the $N = 16$ PD to match $5\times$ the end-customer cost of an AMD Zen4 IO die [4].

Our cost model incorporates adjustments for yield estimation based on critical silicon area, economies of scale via wafer volume discounts, and non-die costs. Specifically, we model yield based only on the area used for logic and IO pads. Non-die costs include expenses related to mask set creation, wafer probing and testing, packaging materials, and

assembly. These costs are assumed proportional to overall die area.

The total cost per die, C_{die} , is calculated as follows:

$$C_{\text{die}} = \frac{C_{\text{wafer, effective}}}{Y_{\text{eff}}} + C_{\text{non-die}}$$

where:

- $C_{\text{wafer, effective}}$ is the wafer cost after applying volume discounts or surcharges.
- Y_{eff} is the yield based on critical area.
- $C_{\text{non-die}} = C_{\text{non-die base}} \times \frac{\text{Total Area}}{\text{Area}_{\text{base}}}$, where $C_{\text{non-die base}}$ is the baseline non-die cost and $\text{Area}_{\text{base}}$ is the area of the small 2-port PD.

Our baseline cost model used in Table 1, the evaluation (Section 7), and Figure 9 all assume that for the 16-ported PD effective wafer costs and non-die costs are equal, i.e.,

$$C_{\text{wafer, effective}} = C_{\text{non-die}}$$

Figures ?? and 16 show what happens if we scale wafer costs by $2\times$ and $\frac{1}{2}\times$, respectively.

C Proof of Pooling Optimality Theorem

Proof sketch. In a fully-connected topology, any set of host demands can be satisfied as long as there is enough total memory capacity across all pooling devices. This is because each host is connected to all pooling devices and can therefore access all available memory capacity. However, in a minimally-connected topology, it may not be possible to satisfy a set of host demands even if there is sufficient total memory capacity across all pooling devices. This can happen if there is a subset of hosts whose total demand exceeds the total capacity available across pooling devices "spanned" by these hosts. The crux of the proof lies in establishing a lower-bound on the total memory capacity available to any subset of hosts of a given size. To do so, we use a counting argument combined with a Cauchy-Schwarz inequality while exploiting the property that every pair of hosts shares exactly one common pooling device. This gives us a lower-bound on the number of pooling devices spanned by a subset of hosts (and therefore memory capacity available to these hosts) as a function of the size of the subset. Now, if the subset of hosts with the k highest demands have total demand less than or equal to the memory capacity specified by the lower-bound for the size k , then it is guaranteed that any subset of hosts of size k will also have total demand less than or equal to the memory capacity available in pooling devices spanned by them. If this condition is true for all k , then all subsets of hosts have access to enough capacity to satisfy their demands (formally, this can be shown by modeling the topology as a flow network and applying the max-flow min-cut theorem).

Definition C.1. A topology is defined as a bipartite graph where one partition consists of hosts and the other partition consists of pooling devices. There is an edge between a host

and a pooling device if and only if the host is connected to the pooling device.

Definition C.2. In a topology, let S be a subset of hosts. $\Gamma(S)$ is the subset of all pooling devices connected to by any host in S .

Definition C.3. $TopoMin(X, N)$ is a minimally connected topology with host port count X and pooling device port count N . The topology satisfies the property that any pair of hosts connects to exactly one common pooling device. A corollary of this property is that the number of hosts is $H = 1 + X(N - 1)$ and the number of pooling devices $M = \frac{H \cdot X}{N}$.

Lemma C.4. Given a set of host memory capacity demands D_1, D_2, \dots, D_H , a topology can satisfy all of these demands if, for every subset of hosts S , $\sum_{i \in S} D_i \leq |\Gamma(S)| \cdot P$, where P is the memory capacity of each pooling device.

Proof. Given a topology and a set of demands D_1, D_2, \dots, D_H , we can construct an equivalent flow network: there is a source node, sink node, a node for each host, and a node for each pooling device. the source node is connected to host node i , with a link of capacity D_i . For every pair of connected host and pooling device in the topology, we add a link between the corresponding host node and pooling node with infinite capacity. Each pooling node is connected to the sink with a link of capacity P (per pooling device memory capacity).

Notice that, a given set of demands can be satisfied by a topology only if the max flow in the corresponding flow network (as constructed above) equals $\sum_i D_i$. By max-flow min-cut theorem, this is equivalent to the min-cut capacity in the flow network being $\sum_{i=1}^H D_i$ (that is, the cut where all nodes are separated from the source). Consider any finite-capacity cut that includes a non-empty subset (S) of host nodes: all the pooling device nodes spanned by this set of source nodes (that is, $\Gamma(S)$) also need to be part of the cut (otherwise the cut capacity would be infinity). The capacity of such a cut would therefore be the sum of D_i for $i \notin S$ plus $|\Gamma(S)| \cdot M$. This capacity can be less than $\sum_i D_i$ only if $\sum_{i \in S} D_i > |\Gamma(S)| \cdot P$. Hence, if $\sum_{i \in S} D_i \leq |\Gamma(S)| \cdot P$ is true for all subsets of host nodes, then all finite-capacity cuts will have capacity greater than or equal to $\sum_i D_i$, which implies that all the demands can be satisfied. \square

Lemma C.5. In $TopoMin(X, N)$, for any subset of hosts S of size k , the following holds:

$$|\Gamma(S)| \geq \frac{k \cdot X^2}{X + k - 1}$$

Proof. For a given subset of hosts S of size k , the total number of outgoing edges from this set is $k \cdot X$. For $j \in \Gamma(S)$, the n_j be the number of edges from pooling device j to any host in S . Clearly $\sum_j n_j = k \cdot X$.

The total number of host pairs in S is $\binom{k}{2}$. The number of host pairs covered by each $j \in \Gamma(S)$ is $\binom{n_j}{2}$. Given the

connectivity property of $TopoMin(X, N)$: since every pair of hosts have exactly one common pooling device, two pooling devices cannot share the same pair of hosts. As a result, the following must hold:

$$\sum_{j \in \Gamma(S)} \binom{n_j}{2} = \binom{k}{2}$$

Simplifying and re-arranging the above, we get:

$$\sum_j n_j^2 = \sum_j n_j + k(k - 1)$$

By cauchy-schwarz inequality, we have $\sum_j n_j^2 \geq \frac{(\sum_j n_j)^2}{|\Gamma(S)|}$. Combining this with the above, we get:

$$\sum_j n_j + k(k - 1) \geq \frac{(\sum_j n_j)^2}{|\Gamma(S)|}$$

Substituting $\sum_j n_j = k \cdot X$ and re-arranging gives the inequality in the lemma statement. \square

Theorem C.6. Given a set of host memory capacity demands D_1, \dots, D_H , let μ be the average memory demand across hosts ($\mu = \sum_{i=1}^H D_i / H$) and let $D_{(1)}, D_{(2)}, \dots, D_{(H)}$ be the host demands sorted in non-increasing order. Memory capacity required by $TopoMin(X, N)$ will be at most α times larger than the memory capacity required by a fully-connected topology (with the same number of hosts), if the following condition is satisfied for all $k = 1..H$:

$$\sum_{i=1}^k D_{(i)} \leq \alpha \cdot \frac{k \cdot N \cdot X}{X + k - 1} \mu$$

Proof. If the condition in the theorem statement is true, then the following holds for any subset of hosts S of size k (because $\sum_{i \in S} D_i \leq \sum_{i=1}^k D_{(i)}$):

$$\sum_{i \in S} D_i \leq \alpha \cdot \frac{k \cdot N \cdot X}{X + k - 1} \mu$$

Substituting $N = \frac{H \cdot X}{M}$ in the above, we get:

$$\sum_{i \in S} D_i \leq \frac{k \cdot X^2}{X + k - 1} \left(\frac{\alpha \cdot \mu \cdot H}{M} \right)$$

For $TopoMin(X, N)$, applying Lemma C.5 to the above, we get:

$$\sum_{i \in S} D_i \leq |\Gamma(S)| \left(\frac{\alpha \cdot \mu \cdot H}{M} \right)$$

By Lemma C.4, the above implies that, $TopoMin(X, N)$ can satisfy all the demands with memory capacity of $P = \frac{\alpha \cdot \mu \cdot H}{M}$ per pooling device. So the total memory capacity that $TopoMin(X, N)$ needs is at most $\alpha \cdot \mu \cdot H$, which is α times the memory capacity needed by a fully connected topology with H hosts. \square